



MASTERARBEIT

Titel der Masterarbeit

The initial steps of autophagy – Atg1 and its targets

Verfasserin

Isabella Hansmann Bakk. rer. nat.

angestrebter akademischer Grad

Master of Science (MSc)

Wien, 2012

Studienkennzahl lt. Studienblatt:

A 066 834

Studienrichtung lt. Studienblatt:

Masterstudium Molekulare Biologie UG2002

Betreuerin / Betreuer:

Prof. Gustav Ammerer

Table of Contents

Abstract.....	4
Zusammenfassung	5
Introduction	6
Autophagy: a major degradation pathway and effective survival strategy.....	6
Mechanism of autophagy in yeast.....	7
The initial stages	8
The late stages of autophagy	10
Cvt-pathway	11
Atg1 kinase complex	12
Atg9.....	13
Atg2 – Atg18 complex	14
Comparison of mammalian autophagy to yeast.....	15
Autophagy and disease.....	17
Methodic issues	19
Current state of the art: Atg1, Atg2, Atg9 and Atg18	19
Protein modification: Mass spectrometry.....	19
Protein interaction: M-track.....	20
Aim of Thesis	22
Material and Methods	23
Primer	23
Strains.....	24
Plasmids	24
Strain construction	25
Plasmid construction	25
SILAC labeling	26
Purification of HTB _{eq} tagged proteins.....	26

Sample preparation for the M-track.....	27
Immunoblotting for the M-track	27
Results.....	28
Mass spectrometric analysis of Atg9 phosphorylation sites in logarithmic growing cells and autophagy inducing conditions	28
Comparison of Atg9 phosphorylation sites in Atg1 wild type and <i>atg1</i> Δ background gives first evidence for Atg1 dependent sites.....	29
Identification of Atg1 dependent sites in Atg9 via SILAC experiments.....	31
Proposed kinase defective mutant Atg1 ^{K54A} still posses kinase activity	36
Characterization of the Atg9-Atg1 interaction via enzymatic tagging	37
Mass spectrometric analyses of Atg2.....	40
Identification of Atg1 targeted sites in Atg2 via quantitative mass spectrometry	42
Determining a possible interaction between Atg1 and Atg2 - preliminary data	46
Mass spectrometric analysis of Atg18 – preliminary data	47
Examination of a possibly interaction between Atg1 and Atg18 – preliminary data ...	48
Definition of an Atg1 consensus motif <i>in vivo</i>	49
Discussion	54
Validation of Atg1 dependent phosphorylation sites on target proteins via mass spectrometry and protein-protein interaction studies	54
Does Atg1 directly interact with its putative targets?	56
Atg1 ^{K54A} defective mutant still possesses some level of activity.....	57
Outlook.....	57
Acknowledgements	59
Literature.....	60
Curriculum vitae	66

Abstract

Autophagy is a degradation pathway of organelles and long lived proteins which becomes activated upon starvation conditions in all eukaryotes. Previous studies have validated the key role of the protein kinase Atg1 in the activation of autophagy; however, so far no targets have been described. Recently, a consensus motif for sites that are modified by Atg1 has been determined by *in vitro* kinase assays and bioinformatic analyses. Furthermore, the autophagy related factors Atg2, Atg9 and Atg18 have been proposed as putative Atg1 substrates. Here we present an approach to validate these observations *in vivo*. To do so, we used mass spectrometry and a novel protein-protein proximity assay and that based on stable enzymatic modifications. Our analysis showed that Atg9 and Atg2 are indeed substrates of Atg1. Moreover, we defined an Atg1 consensus motif based on *in vivo* data.

Zusammenfassung

Autophagie ist ein eukaryotischer Abbaumechanismus für langlebige Proteine und Organellen, der unter nährstoffarmen Bedingungen hochreguliert wird. Vorangehende Studien bestätigten bereits die Schlüsselfunktion der Atg1 Kinase in der Aktivierung von Autophagie. Bisher wurden allerdings noch keine Substrate von Atg1 beschrieben. Vor kurzem wurde eine Konsensussequenz für durch Atg1 modifizierte Peptide mittels *in vitro* Methoden definiert. Dies ermöglichte die Identifizierung von Atg2, Atg9 und Atg18 als wahrscheinliche Substrate der Atg1 Kinase. In dieser Arbeit präsentieren wir einen Ansatz um diese Hypothese mit *in vivo* Methoden zu bestätigen. Dafür verwendeten wir quantitative Massenspektrometrie und einen neuen Protein-Protein Interaktionsassay, der auf sogenanntem „enzymatischem Tagging“ basiert. Unsere Experimente zeigen, dass Atg9 und Atg2 Substrate von Atg1 sind. Zusätzlich konnten wir eine auf unseren *in vivo* Daten basierende Atg1 Konsensussequenz definieren.

Introduction

Autophagy: a major degradation pathway and effective survival strategy

Survival of a cell strongly depends on the supply of nutrients from the environment to provide energy and components for the maintenance of essential life processes. However, cells are frequently exposed to adverse conditions, such as starvation. To address this problem, eukaryotes have evolved different surviving strategies, one of which is called autophagy. Autophagy is defined as a degradation mechanism recycling cellular components that appear in excess and are not required for the momentary physiological situation. Degradation of these components makes these building blocks available for essential metabolic functions. Therefore, the main function of autophagy is the supply of amino acids under low-nutrition conditions, such as starvation and stress conditions. Consequently, this catabolic process is highly activated during starvation, but also during hypoxia, intracellular stress, exposure to high temperature, high culture density and hormone or growth factor deprivation [1]. In addition, autophagy is important for the clearance of damaged or unnecessary products from cells. Thus, autophagy is also active at basal levels during logarithmic growth. It is the only known mechanism for the degradation of long lived proteins and organelles, a property that makes autophagy important for the homeostasis of cellular components.

Three major types of autophagy have been defined so far, all of which are essential for both, starvation conditions and cellular homeostasis: (1) chaperone mediated autophagy, (2) microautophagy and (3) macroautophagy. These three types differ in their sequestration and delivery mechanisms. In contrast to the last two types chaperone mediated autophagy has only been observed in higher eukaryotes. A chaperone forms a complex with the substrate proteins which are identified via a specific recognition sequence. This chaperone-substrate complex localizes to the lysosome, where target proteins become imported via a lysosomal membrane receptor called Lamp2 [2]. Because the amount of Lamp2 bound to the lysosomal membrane is limited, chaperone mediated autophagy is the only type of autophagy for which saturation has been described.

Microautophagy is defined as the direct engulfment of substrates by the lysosome or the vacuole. Similar to the chaperone mediated autophagy, this process also involves a chaperone complex and in addition parts of the conventional machinery defined by the Atg proteins (see below). Different subtypes such as micropexophagy, piecemeal microautophagy of the nucleus and micromitophagy have been described [3].

The third type of autophagy, which is subject of this thesis, is called macroautophagy. Macroautophagy is often and hereafter only referred to as autophagy. Autophagy is defined as sequestration of cytoplasmic material by double-membrane vesicles and the subsequent degradation of the contents in the vacuole or the lysosome. Because this sequestration of cytoplasmic material is an unspecific process, the term bulk autophagy is also often used. However, selective subtypes macroautophagy also exist, the most prominent of which are mitophagy, pexophagy, reticulophagy, lipophagy and the Cvt-pathway, the latter is a special subtype of autophagy found in yeast [4,5].

Mechanism of autophagy in yeast

Autophagy is a mechanism conserved in all eukaryotes although individual variations have been described in different organisms. So far, most of the insights about the factors involved in autophagy have been gained by studying this process in the yeast *Saccharomyces cerevisiae*. Furthermore, all essential factors found in yeast have homologues in higher mammals. Therefore, *Saccharomyces cerevisiae* is a suitable organism to study autophagy.

The process of autophagy is mainly accomplished by autophagy related genes (ATG); so far 33 ATG genes have been identified. The core machinery, which is needed for the bulk autophagy as well as for selective types of autophagy, consists of 17 proteins encoded by these autophagy related genes. The most important key regulator of the initial steps of autophagy is the Atg1 kinase [4].

Autophagy can be classified in four stages: (1) the formation of a phagophore at the phagophore assembly site (PAS), (2) the expansion of the phagophore to sequester the cargo into autophagosome, (3) the fusion of the autophagosome with the vacuole or lysosome to release the autophagic body and (4) at last the degradation by vacuolar hydrolases and the release into cytosol by various permeases [4] (see Figure 1).

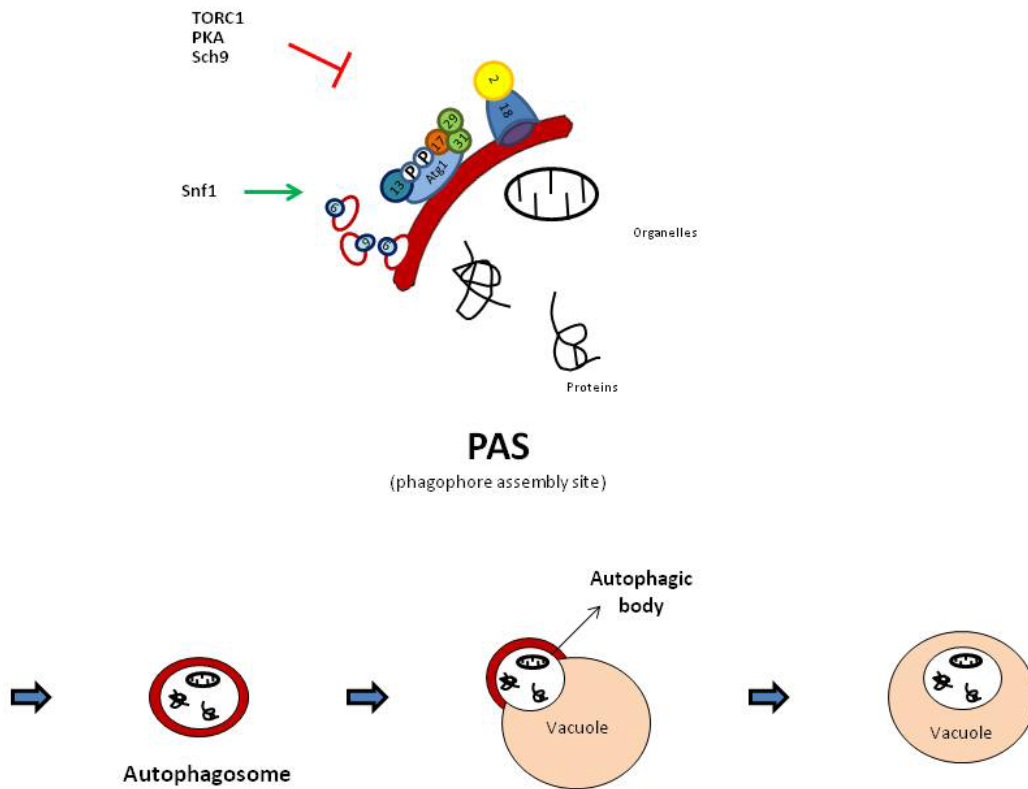


Figure 1. **The actual model of autophagy.** In the early stages of autophagy protein complexes like the Atg1 kinase complex or the Atg2-Atg18 complex localize to the PAS (Phagophore Assembly Site) to recruit other Atg proteins and form autophagosomes. The completed autophagosome is transported to the vacuole, where its outer membrane fuses with the vacuole to release the autophagic body. In the lumen the autophagic body is degraded and the degradation products are released into the cytosol.

The initial stages

The initiation of autophagy in yeast is affected by positive and negative regulators (reviewed by Cebollero and Reggiori, 2009) [6]. Negative regulators are the TOR (target of rapamycin) kinase complex 1 (TORC1) and Sch9 kinase of the nitrogen sensing and signaling systems, and the cAMP-dependent protein kinase A (PKA) of the glucose signaling systems. In contrast, the AMP dependent kinase Snf1 has been described as a positive regulator of autophagy. However, the details about the sensing of the extracellular nutrient levels by Tor are still unknown. In contrast to mammals, two homologues of Tor, namely Tor1 and Tor2, have been described in yeast. Both are required for the assembly of TORC1 that is inhibited through rapamycin, whereas only Tor2 is necessary for the rapamycin insensitive TOR complex 2 (TORC2). During nutrient rich conditions TORC1 is thought to inhibit autophagy by direct phosphorylation

of Atg13. TORC1 has also been described to indirectly influence autophagy via Sch9 and PKA. However, recent evidence suggests that PKA signaling is not influenced by rapamycin and therefore by TORC1 signaling (W. Reiter personal communications). Nevertheless, PKA and Sch9 also regulate autophagy independent of TORC1. Sch9 is the homologue of Akt and S6K in yeast. Details on how Sch9 inhibits autophagy are still not known.

PKA responds to the availability of carbon sources. In the presence of glucose the GTPases Ras1 and Ras2 are activated. Subsequently, the two proteins bind to the adenylate cyclase Cdc35 and thereby stimulate cAMP synthesis. Elevated cAMP levels lead to the activation of PKA which in turn attenuates autophagy. It has been suggested that this inactivation is mediated by PKA dependent phosphorylation of Atg1, Atg13 and Atg18 [7,8]. The positive regulator Snf1 is the homologue of the mammalian AMPK, and Atg1 and Atg13 have been described as putative direct targets of Snf1 in yeast. Furthermore, the regulation of autophagy by Snf1 might also occur on a transcriptional level [9,10].

All positive and negative signaling inputs become integrated at the level of the key regulator kinase Atg1. Atg1 appears in two different complexes; the first complex includes Atg13, Atg17, Atg29 and Atg31 and is specific for autophagy (see Figure 2) [11-13]. During nutrient rich conditions Atg13 is hyperphosphorylated, which leads to a low binding affinity for Atg1. Upon activation the phosphorylation pattern of Atg13 becomes altered which allows association with Atg1 and Atg17 and thereby promoting Atg1 activation. The assembly of the complex is important for its localization to the PAS where the Atg1 kinase can execute its activity. [5,11,14].

A second important complex including the phosphatidylinositol 3-kinase Vps34 is required for the expansion of the phagophore and the completion of the autophagosome. Vps34 is required for the recruitment of phosphatidylinositol 3-phosphat (PtdIns(3)P) binding proteins to the PAS. Vps34 is the only phosphatidylinositol 3-kinase in yeast and consequently this kinase can be found in two different complexes, one specific for endosomal protein sorting and one for autophagy. The autophagy specific complex consists of Vps15, Vps34, Atg6 and Atg14. Vps15 is necessary for association of the complex to the membrane and Atg14 determines the specificity for autophagy. Once the complex is assembled it localizes to the PAS, where Vps34 phosphorylates the phagophore. As a consequence PtdIns(3)P binding proteins like Atg18, Atg20, Atg21 and Atg24 become recruited. Of these PtdIns(3)P binding

proteins only Atg18 is essential for the autophagosome formation [15]. Atg18 forms a complex with Atg2 and its PtdIns(3)P binding ability is needed for the localization of Atg2 to the PAS. However, the exact function of this complex remains subject to further investigations [16].

A very important and frequently discussed question concerning the initial steps of autophagy asks about the origin of the autophagic membranes. So far the origin itself has not been identified yet. Nevertheless, many studies have shown the importance of Atg9 for the delivery of the membrane components to the PAS. Atg9 is the only indispensable transmembrane protein during initiation of autophagy and the only one which is conserved across species [17]. Atg9 cycles to and from the PAS and this cycling is essential for the phagophore formation. In *atg1Δ*, *atg2Δ* or *atg18Δ* single deletion strains Atg9 accumulates and remains at the PAS, which consequently leads to defective autophagy. Moreover, Atg9 and Atg1 are individually recruited to the PAS and thereby initiate the recruitment of the Atg18-Atg2 complex. Taken together the deletion of *atg1Δ*, *atg2Δ* or *atg18Δ*, which causes a defect in autophagy, indicates the importance of the retrograde transport (from PAS to its peripheral localization sites) of Atg9 [18].

Two ubiquitin like proteins (Ubl) are involved in the completion of the autophagosome, namely Atg8 and Atg12. Both are believed to be involved in the membrane expansion of the phagophore [19]. Atg8 binds to the phosphatidylethanolamine (PE) of the autophagic membranes [5]. In course of that the C-terminus of Atg8 has to be cleaved by the protease Atg4 [20], allowing Atg8 to bind to PE with the help of E1-like activating enzyme Atg7 and E2-like conjugating enzyme Atg3 [21]. Similarly, the Ubl protein Atg12 forms with Atg5 an E3 like conjugate through the help of Atg7 [22] and the E2 like enzyme Atg10 [23]. Subsequently, Atg16, which is necessary for the localization of this complex to the outer autophagic membranes, associates with Atg5 [24]. The Atg12-Atg5-Atg16 complex is also involved in the conjugation of Atg8 to PE [25]. The recruitment of the two ubiquitin like proteins is dependent on Atg9 and the Vps34 complex [19].

The late stages of autophagy

The targeting of autophagosome to the vacuole and its subsequent fusion requires for the following factors: target SNAP receptor (t-SNARE) Vam3, the vesicle SNAP receptor (v-SNARE) Vti, the GTPase Ypt7 and ATPase Sec18, a protein from the

secretory pathway [26-29]. The detailed course of events is to date only poorly understood. However, autophagy is known to utilize the general vesicle trafficking machinery, although the system is modulated differently for the use of autophagy [30].

The last stages of autophagy, the vesicle breakdown and release of the autophagic degradation product, are also not understood in detail. To date only one lipase for the breakdown of the autophagic body, namely Atg15, has been identified [31]. Furthermore, Atg22, a leucine effluxer, is the only proof of a permease for the transport of degradation products into the cytosol [32].

Cvt-pathway

The cytoplasm to vacuole targeting (Cvt)-pathway is a special subtype of autophagy that is only found in yeast. The Cvt-pathway sequesters vacuolar hydrolases that are not derived from the secretory pathway like Ape1 (aminopeptidase1) and Ams1 (α -mannosidase). Via Cvt-vesicles these hydrolases are transported to the vacuole where these enzymes become activated via proteolytic cleavage [4,33,34]. Other recently discovered cargos are Ape4 (aspartyl aminopeptidase) and Lap3 [35,36].

Although, the main function of the Cvt pathway is not the degradation of proteins it is considered to be a subtype of autophagy since the same machinery is involved. The Cvt pathway is active even under nutrient rich conditions. During starvation the machinery switches to autophagy. Of all 33 known Atg proteins 16 are employed by the Cvt-pathway to determine its specificity and 17 are used by both bulk autophagy and the Cvt-pathway. For example, Atg1 appears in two different complexes [4]. These two different Atg1 complexes are important for the switch of the Cvt-pathway during nutrient rich conditions to autophagy during starvation conditions which is mediated via the TORC1 complex. The core compounds of these complexes, consisting of Atg1 and Atg13, are the same for autophagy and the Cvt-pathway but additional factors like Atg11, Atg20 and Atg24 are required to specify this complex for the Cvt-pathway (see Figure 2) [11,37]. However, the main difference of the Cvt-pathway to autophagy is the selective sequestering of the cargo molecules [4].

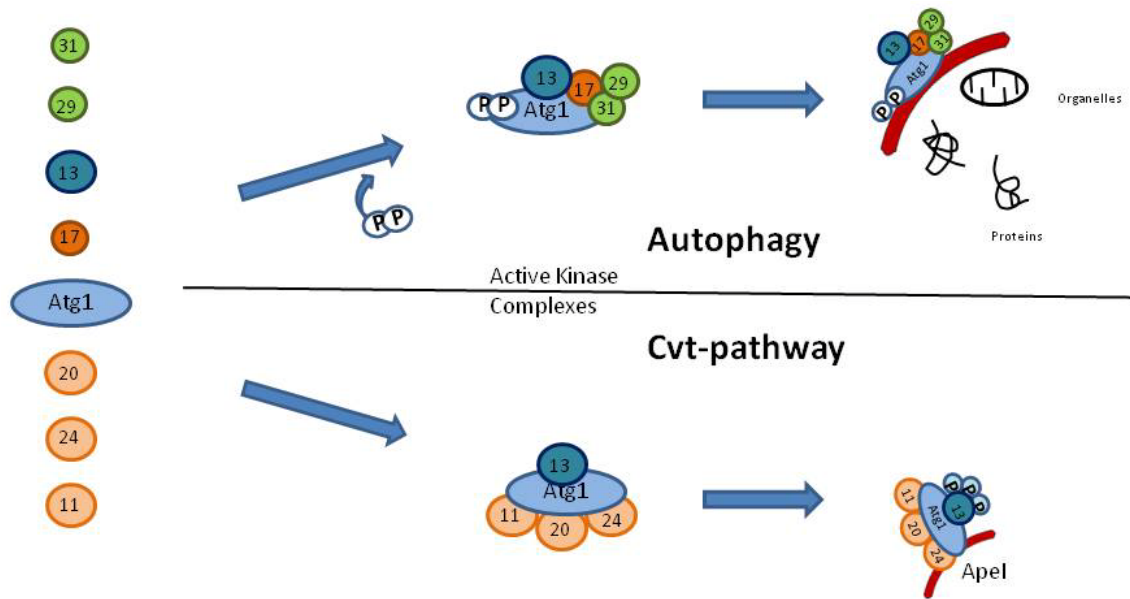


Figure 2. **The different composition of the Atg1 complex in autophagy and the Cvt-pathway.** This figure shows the important factors involved in the assembly of the active kinase complexes (factors that are not needed for the Cvt-pathway or autophagy are not shown). The active Atg1 kinase complex differs between autophagy and the Cvt-pathway in its constituting proteins and phosphorylation state.

Atg1 kinase complex

Atg1 is a serine/threonine protein kinase [38] and has been described as key regulator of autophagy. As mentioned above, Atg1 becomes activated by binding of Atg13 in response to starvation conditions or rapamycin treatment. This association with Atg13 leads to the additional interaction of Atg1 with Atg17 [11], which consists as a ternary complex with Atg29 and Atg31. Atg29 and Atg31 are responsible for the PAS localization of the Atg1 kinase complex, a necessary event for the recruitment of other Atg proteins and the formation of autophagic membranes. Nevertheless, it has been reported that Atg1 kinase activity itself is not connected to PAS localization of the complex or the reception of the nutrient signal. If this is true the kinase activity would be only essential for the phosphorylation of specific substrates at the PAS[11,12].

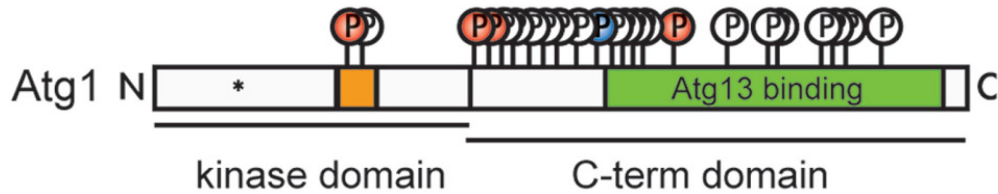


Figure 3. **Atg1 phosphorylation sites.** The activation loop is marked in orange. Phosphorylation sites upregulated after treatment with rapamycin are shown in red, downregulated sites are shown in blue. (Figure taken from Kijanska *et al.*) [39].

Atg1 is a 101,7 kDa protein containing a domain for interaction with Atg13 on the C-terminal half and an activation loop between DFG (aspartate-phenylalanine-glycine) and APE (alanine-proline-glutamate) motifs in the kinase domain at the N-terminal half (see Figure3). In *Saccharomyces cerevisiae* several post translational modifications on Atg1 have been reported [39,40]. Importantly, these studies showed that T226 and S230 of the activation loop become phosphorylated upon starvation conditions or rapamycin treatment and this dual phosphorylation is important for the activation of the kinase. Both residues, T226 and S230, are highly conserved between activation loops of all Atg1 homologues. Furthermore, Yeh *et al.* reported that T226 becomes modified by autophosphorylation. However, it is still unclear whether this autophosphorylation event becomes activated in *cis* or *trans*. The importance of these sites for the activity of the kinase was confirmed via point mutations, which resulted in defective Apel processing and defective Atg8-GFP accumulation in the vacuole. Furthermore, phosphorylation at these two sites enhances the Atg1 kinase activity but are not important for the assembly of the Atg1 complex or the PAS localization [39]. Additionally, Kijanska *et al.* identified additional rapamycin regulated sites (S351, S356, S533 and S474) on Atg1 and confirmed the *in vivo* phosphorylation of two postulated PKA sites (S505 and S515) by quantitative mass spectrometry. However, the function of these phosphorylations still remains elusive.

Atg9

Atg9 is the only transmembrane protein that is essential for autophagy. Its function is supposed to be the delivery of membrane components to the forming autophagosome [4]. He *et al.* showed that Atg9 is able to interact with itself, and that this interaction is necessary for the anterograde (from cytosol to PAS) transport of Atg9 [41]. In logarithmic growing conditions Atg9 is found in punctate structures throughout the

cytosol. In autophagic conditions Atg9 starts to cycle to the PAS, which is essential for membrane formation [18]. Many microscope studies showed that the majority of the Atg9 containing puncta colocalize with mitochondria [42,43]. However, these puncta near the mitochondria are independent clusters [43]. Indeed, the origin of the membranes is still debated and the possibility that Atg9 comes from the Golgi-endosomal system still exists [44]. While the Atg9 transport to the PAS in the Cvt-pathway depends on Atg11 and the actin cytoskeleton [45], the anterograde transport during autophagy is supported by the peripheral membrane protein Atg23 and the transmembrane protein Atg27 [46,47]. Nevertheless, Atg23 and Atg27 only influence the efficiency of the process [48].

Furthermore, as already mentioned above, the retrograde transport of Atg9 depends on the PAS localization of the Atg13- Atg1 complex, the Vps34 complex, the Atg2-Atg18 complex as well as on the binding ability of the Atg2-Atg18 complex to Atg9 [18,49].

Atg2 – Atg18 complex

After induction of autophagy Atg2 and Atg18 form a complex. Atg18 possesses a PtdIns(3)P binding motif consisting of FRRG (phenylalanine, arginine, arginine, glycine) and thereby the Atg2-Atg18 is recruited to the phagophore via the Vps34 complex, which specifically phosphorylated the phosphoinositides of the autophagic membranes [16]. Furthermore, Atg18 can also bind PtdIns(3,5)P₂, but it was suggested that this feature is not important for autophagy [50]. Moreover, Obara *et al.* bypassed the requirement of Atg18 for PAS localization of Atg2 by adding a 2xFYVE (phenylalanine, tyrosine, valine, glutamine) domain (a specific PtdIns(3) binding domain) directly to Atg2. However, cells containing Atg2 with this PtdIns(3)P binding motif were still unable to overcome their defect in autophagy. Therefore, Obara *et al.* proposed that, besides the localization of the Atg2-Atg18 complex, Atg18 has an additional role in autophagy [16].

However, speculations about the involvement of the Atg2-Atg18 complex in the retrograde transport of Atg9, the generation of the negative curvature of the phagophore, the construction and maintenance of the elongating edges of the expanding membrane [16] or a role for Atg8 protection from unregulated cleavage by Atg4 [51] still need to be proven.

Atg2 is a poorly characterized protein. Deletion studies performed by Reggiori *et al.* show that Atg2 is essential for autophagy and further propose a role of Atg2 in the retrograde transport of Atg9 [18]. The Atg2 recruitment to the PAS by Atg18 and subsequently its function is disturbed in Atg1, Atg6, Atg9 and Atg14 deficient cells [52]. Nevertheless, the exact role of Atg2 needs to be determined.

Comparison of mammalian autophagy to yeast

As described above many autophagy related factors are highly conserved between eukaryotes. Therefore, many similarities in the mechanism of autophagy between mammals and yeast can be expected. However, autophagy in mammals still remains a poorly characterized subject; therefore this chapter shall only give an overview about the similarities and differences to yeast (as far as examined).

For instance, autophagy in mammalian organisms is also regulated by AMPK and mTORC1 signaling. Mammals have two Atg1 kinase homologues, Ulk1 and Ulk2, but only Ulk1 is essential for autophagy [53-55]. During starvation the AMPK kinase phosphorylates Ulk1 on S317 and S777, thereby leading to the initiation of autophagy. During adequate nutrition conditions mTORC1 phosphorylates S757 of Ulk1, which leads to interference for the interaction of AMPK with Ulk1 and causes the inhibition of autophagy [56].

The enhancement of the Ulk1 kinase activity, as well as the localization of Ulk1 to the phagophore requires the formation of the Ulk1 kinase complex harboring two other proteins, mAtg13 and Fip200, the respective homologues of Atg13 and Atg17 in *Saccharomyces cerevisiae* [57,58]. In contrast to yeast, phagophore formation takes place at multiple sites in the cytoplasm [30]. Furthermore, regulation of mAtg13 by mTORC1 has also been described in the mammalian system. Though, unlike the situation in yeast, the complex of mAtg13 and Ulk1 is not only found during starvation, these two proteins also interact during rich growth conditions [57,58].

Another essential factor of this complex is the mAtg13 binding protein Atg101, which is thought to protect mAtg13 from proteasomal degradation [57,58].

Recruitment of PtdIns(3)P binding proteins to the PtdIns(3)P on the autophagic membranes requires the activity of Vps34. As in yeast two different PtdIns(3) kinase containing complexes exist, one for autophagy and one for the endosomal protein sorting, the common core complex consists of Vps34, Beclin1 and Vps15. The specificity of this core complex for autophagy is determined by mAtg14 [59].

Additionally, the PtdIns(3) kinase interacting proteins UVRAG (UV radiation resistance-associated gene), AMBRA1 (activating molecule in beclin1-regulated autophagy) and Bif1 (Bax-interacting factor 1) were discovered as positive regulators for autophagy, whereas the interaction with rubicon (RUN domain and dysteine-rich domain containing beclin-1-interacting protein), and the antiapoptotic Bcl-2 family members Bcl-2 (B-cell lymphoma 2) and Bcl-x_L (B-cell lymphoma extra large) inhibits autophagy [60].

The PtdIns(3)P binding proteins in mammals include Alfy (autophagy-linked FYVE protein), DFCP1 (double FYVE domain-containing protein) and the two Atg18 orthologs WIPI1 and WIPI2 (WD repeat proteins interacting with phosphoinositides 1 and 2). The function of WIPI1 and WIPI2 for mammalian autophagy is only partially understood and still needs to be analyzed in detail [30]. However, WIPI1 has been shown to interact with one of the two Atg2 orthologs but colocalizes with LC3 (microtubule-associated protein light chain 3), a homologue of Atg8. WIPI2, which is thought to be the ortholog to Atg21 in mammals, associates indirectly with Atg2a and may be involved in the recruitment of LC3 [61,62]. While the contribution of DFCP1 to autophagy is still unknown, Alfy is at least known to colocalize with Atg5 and LC3 [63].

As in yeast the origin of the autophagic membranes in mammalian cells remains unknown. However, in mammals the cycling of mAtg9 was observed to occur between the trans-Golgi network, the endosomes and the LC3 labeled autophagosomes. mAtg9 cycling depends on ULK1 and the PtdIns(3) kinase [64]. Furthermore, the p38α MAPK (mitogen-activated protein kinase) is known to inhibit autophagy by regulating the interaction of p38IP and mAtg9 [17].

Homologues of both Ubl systems of yeast can also be found in mammals. The mammalian Atg12-Atg5-Atg16L complex has a higher molecular weight than in yeast and the membrane targeting of Atg16L only depends on Atg5 [65]. Nevertheless, the complex requires the Ubl protein Atg12 for the membrane elongation [66]. Additionally, a recent study describes Alfy as a part of this complex [67]. The Ubl protein Atg8 has four homologues in mammalian, namely LC3, GABRAP (γ-aminobutyric-acid type A receptor associated proteins), GATE-16 (golgi-associated ATPase enhancer of 16kDa) and the uncharacterized Atg8L, which are believed to be involved in the completion of the autophagosome. The C-terminus of LC3, GABRAP and GATE-16 is removed by proteolytic cleavage which leads to to exposition of a glycine that allows binding to the PE in the autophagic membranes. In vitro studies provide evidence that the four Atg4 homologues hAtg4A, hAtg4B, hAtg4C and hAtg4D are at least partly responsible for this

cleavage. Atg3 and Atg7 modify these cleaved forms into the membrane bound LC3-II, GABRAP-II and GATE-16-II. LC3-I is the only one that does not localize to membrane compartments before modification [68].

The mechanism for the targeting of autophagosomes to the lysosomes is subject of many recent studies. Kimura *et al.* observed microtubule and dynein-dynactin motor complex dependent the movement of autophagosomes, which is mediated by the LC3. This movement is supposed to be involved in the targeting of the autophagosomes, but whether microtubules prevent the early fusion of immature autophagosomes as suggested by Fass *et al.* or mediates their fusion by targeting the autophagosomes to the lysosomes as proposed by Köchl *et al.* is still not clear. However, microtubules were also found to be involved in the formation of autophagosomes but details about the exact function of this event remain to be examined [69-71].

The study of Gordon and Seglen as well as the study of Dunn proposes that mammalian autophagosomes fuse with endosomal vesicle forming an amphisome (a prelysosomal hybrid organelle) before they fuse with lysosomes [72,73]. The t-SNAREs Vamp3 and GTPase Rab11 are required for the development of amphisomes, whereas the SNAREs VAMP7, VAMP8 and Vti1b as well as Rab7, which depends on the lysosomal membrane proteins Lamp1 and Lamp2, are required for the fusion with the lysosome [74-76]. These proteins were found to be involved in the fusion processes of autophagy but for insights into the exact mechanisms of these fusion processes and the role of these further studies are necessary.

Autophagy and disease

In the early years of autophagy its major role was supposed to be the nutrient supply during starvation but in the recent years connections with lots of cellular processes and diseases have also been reported.

For example, autophagy plays an essential role in the development of the fertilized zygote to the blastocyst. To enable the development of the highly differentiated oocyte into an undifferentiated state after fertilization, degradation of the whole maternal mRNA and proteins is necessary. Tsukamoto *et al.* found evidence that autophagy is involved in this process, since autophagy deficiency is lethal for the zygote. Moreover, in this developmental stage autophagy seems to be important to provide sufficient amounts of amino acids for protein synthesis. Subsequently, in autophagy deficient cells the fertilized zygote could not develop to the blastocyst [77]. Furthermore, other studies

described that autophagy is essential directly after birth, when trans-placental nutrition supply is interrupted [78].

Autophagy was also found to be connected with neurodegenerative diseases. As mentioned above, a major function of autophagy is the turnover of cytoplasmic components to avoid the accumulation of abnormal or damaged proteins. In Atg7 and Atg5 deficient mice an increase of polyubiquitinated proteins in neuronal cells was observed. Autophagy was suggested to be involved in the degradation of these proteins because the proteasome function in these cells was still normal and these two mechanisms form the major degradation pathways of proteins in mammals. The accumulation of these proteins led to behavioral defects, uncoordinated movements and shortened life span [79-81]. Furthermore, a connection to Huntington disease was observed. The cause for Huntington is the accumulation of mutant huntingtin protein in the cell and this accumulation has been shown to be extremely increased in neurons defective for autophagy [80].

Moreover, mutations or downregulation of some ATG genes shorten the life expectancy in lower eukaryotes like yeast, *Caenorhabditis elegans* and *Drosophila melanogaster* and therefore provided a link of autophagy with aging. In aging cells the activity of autophagy decreases thereby leading to a lower clearance of damaged and wrong synthesized components, causing typically age-related phenotypes. In mouse liver cells the observed age-related phenotypes vanished by restoring the defects in autophagy. Additionally, in recent years caloric restriction, which causes higher activity of autophagy, was observed to mediate anti-aging effects. [82].

Autophagy has also been described to be involved in immunity. Autophagy provides cytosolic peptides for antigen presentation on MHC II molecules [83,84]. Furthermore, the Toll-like receptors 4 and 7 apparently can induce autophagy and lead to the destruction of intracellular microorganism [85,86]. Examples for autophagy supporting cellular defense are given by *group A Streptococcus* and *Salmonella typhimurium*, both of them are enveloped by autophagosomes [87,88].

The role of autophagy for cancer development is still ambiguous. Mathew *et al.* discovered that autophagy protects the genome by maintaining metabolism and survival during metabolic stress thereby inhibiting tumor development and Liang *et al.* showed the tumor suppressing effect of the mammalian Atg6 homologue Beclin-1[89,90]. On the contrary Carew *et al.* found that the effect of the anti-cancer drug SAHA is enhanced when autophagy was disrupted [91]. Additionally, it was found that a defect in

autophagy and apoptosis promotes necrotic cell death. Consequently when autophagy is inhibited in starvation the cell death of apoptosis-refractory tumors can be restored, but this necrosis correlated also with inflammation and accelerated tumor growth [92]. This area still requires for more intense investigations to evaluate if there is a clinical possibility to apply autophagy for tumor suppression.

To sum it up, all these examples indicate the importance for further investigations in autophagy and illustrate the growing interest in this subject.

Methodic issues

Current state of the art: Atg1, Atg2, Atg9 and Atg18

As summarized above, there remain many open questions about the mechanism of autophagy. Our research group together with our collaborators focused on the identification of targets of the Atg1 kinase. Through a peptide chip and a subsequent bioinformatic analysis a consensus motif for the Atg1 could be identified. The identification of this motif served as a basis for a scan for proteins carrying putative phosphorylation sites and provided the first hint for Atg2, 9 and 18 to be putative kinase substrates. Moreover, with an *in vitro* kinase assay and point mutations, our collaborators could confirm some of these sites [Claudine Kraft, unpublished data].

These data give strong evidence for the putative targets of the Atg1 kinase complex but since these results were obtained *in vitro* a validation *in vivo* is required. Thus, the aim of my master thesis is the examination of Atg2, 9 and 18 as targets of the Atg1 kinase in the yeast *Saccharomyces cerevisiae*. To do this, we use two different approaches: first, quantitative mass spectrometry and second, a proximity assay, which has been developed in our laboratory and is based on stable enzymatic modifications.

Protein modification: Mass spectrometry

Our mass spectrometric analysis is based on the analysis of modifications of purified proteins of interest. To be able to do this, we use a modified version of the HTB_{eaq} tag which is the established tandem affinity purification system in our lab.

Our HTB_{eaq} tag is a modified version of the tag which has been developed by Tagwerker *et al.* 2006. The tag consists of three elements: two poly-histidin domains followed by three TEV cleavage sites and finally a biotinylation sequence. Nourseothricin is used as a selection marker. By using this tag two purification steps

can be performed. With the poly-histidin domain a rough pre-purification with Ni²⁺ - Sepharosebeads can be performed followed by a more specific purification using the strong interaction of biotin and Streptavidin-Agarose beads [93].

Another important advantage of this tandem affinity purification method is that the procedure is done under denaturing conditions. This is of high importance since posttranslational modifications can be preserved [93].

For quantitative analysis stable isotope labeling with amino acids in cell culture (SILAC) labeling is our method of choice. With SILAC the differences of the proteome of cells under different conditions can be observed. This method is based on the principle that peptides, which are labeled with different stable isotopes, are chemical identical but differ in their mass.

To perform a SILAC analysis a preculture of the cells has to be divided. One half is grown on normal full medium, the other half is supplemented with ¹³C labeled arginine and lysine. SILAC strains are auxotroph for lysine and arginine and therefore have to incorporate these amino acids to be able to grow. However, recent experiments [Verena Unterwurzacher, unpublished data] showed these auxotrophies to be not absolutely necessary for efficient incorporation of many amino acids. In the same environment the cultures incorporate these amino acids in the same amount and thus they are comparable. Only one of the halves becomes treated with the condition of interest (in our case we used rapamycin to induce autophagy) and immediately after harvesting the treated and untreated cells are unified. Next, the proteins are purified and prepared for mass spectrometry. Treatment with trypsin digests the proteins into peptides of different sizes, each carrying arginine or a lysine at the C-terminal end. Consequently, they are labeled with a heavy or light amino acid. The resulting heavy to light ratio gives information about relative differences in the abundant peptides. [94].

Protein interaction: M-track

As described above activation of autophagy requires dynamic interaction of a variety of different factors. We wanted to study these protein-protein interactions using an assay based on enzymatic tagging. Enzymatic tagging is defined as a transfer of a chemical modification between protein tags that can easily be detected with an appropriate readout system. I made use of the so called M-track that has been developed in our research group, to study the binding of Atg1 to its putative targets Atg2, Atg9 and Atg18. For the M-track the two proteins of interest had to be tagged with either a hyperactive

catalytic domain of the murine histone methyltransferase (HMT) Suv39h1 (donor) or a region of the first 21 amino acids of histone3 containing lysine 9 (our tag contains four copies of this 21 amino acid region), which is a substrate of the HMT. Additionally, the histone tag also contains three HA-epitopes, which are used for loading control. Depending on the strength of the interaction, lysine 9 either becomes mono-, di- or trimethylated by the HMT (see Figure 3). For each of these types of modification a specific monoclonal antibody exists.

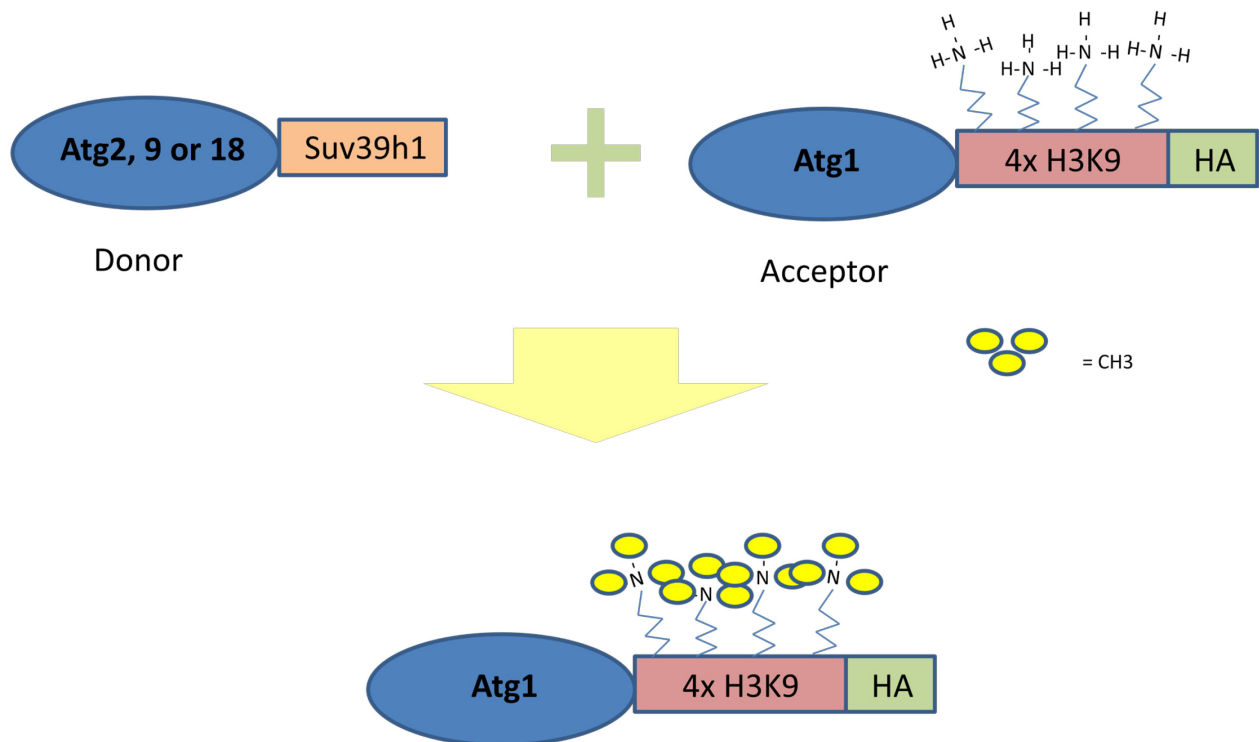


Figure 3. **A schematic illustration of the mechanism of the M-track.** When the two proteins of interest interact the Acceptor becomes methylated through the Donor. Each lysine 9 of the four histone 3 tags can be mono-, di- or trimethylated (here only trimethylation is shown).

One major advantage of enzymatic tagging is that it allows examination of interactions of membrane and membrane associated proteins like Atg2, Atg9 and Atg18. Furthermore, the method allows detection of transient interactions. Interactions can be observed at endogenous protein levels. Finally, quantification of the methylation signal is also possible. [Zuzuarregui *et al.*, manuscript submitted (Nature), I. Dohnal and C. Friedmann, PhD thesis]. Once this assay is established for Atg1 proteins it will provide many possibilities: For example the interaction can be studied in ATG deletion mutant strains to assess the importance of other factors on a specific interaction. Furthermore,

interaction of point mutations at specific phosphorylation sites can be studied to examine the effects of specific signaling cascades.

Aim of Thesis

This thesis is based on recently published Atg1 phosphorylation studies of Kijanska *et al.* and Yeh *et al.* These phosphorylation analyses emphasized the key role of the Atg1 kinase as mediator between nutritional signaling and autophagy. Lots of efforts have been undertaken to identify the different signaling inputs for the Atg1 kinase. Also the consequences of the activation of the kinase have been thoroughly studied. However, the direct targets of the kinase have not been identified yet. Our collaboration partner, Claudine Kraft, identified putative targets of the Atg1 kinase by *in vitro* methods and examined whether Atg1 can still phosphorylate point mutated variants of these putative targets by *in vitro* kinase assays. The aim of the thesis presented here is the validation of the putative Atg1 targets, Atg2, Atg9 and Atg18, by *in vivo* methods such as quantitative mass spectrometry. With this method we can identify the exact sites that are regulated by the kinase Atg1. A second approach focused on the establishment of the M-track assay, an enzymatic tagging system that was established in our laboratory to examine protein-protein interactions. This *in vivo* method will allow us to confirm that Atg1 directly interacts with its targets. Furthermore, by using deletion mutants that inactivate the Atg1 kinase complex it will allow us to study the dependency of the interaction on the activity of the Atg1 kinase.

Material and Methods

Primer

Atg1_sphI_fw1	GTAGGCATGCACCTGCCACAAGGTTATTTCTACAC
Atg1_bgIII_re1	GTCGAGATCTGCTTTAGCGTTATATTTTTGATAATTC
Atg1_bgIII_fw2	GTCGAGATCTGTGGTCTGTCCGTACAGTGGTATTCCG
Atg1_xbaI_re2	GGCGTCTAGAATTTTGGTGGTTCATCTTCTGCCTC
Atg18_sphI_fw	GTAGGCATGCATATATGGTGATATGAATGGCCACC
Atg18_link_xbaI_re	GGCGTCTAGAGGACCCACCACCTCCAGAGCCACCGCCACCATC CATCAAGATGGAATACTGTGAC
Atg9_sphI_fw1	GTAGGCATGCCGGATTGAACAGTTATTCCCTGTGAGAC
Atg9_agel_re1	GTCGACCGGTAAACCGAGGTTGTGTAGCACTACCAAAG
Atg9_agel_fw2	CTGCACCGGTTCCGCCCTTAAATAATAACAAACAGGTTCCAC
Atg9_xbaI_re2	GGCGTCTAGATCTTCCGACGTCAGACTTCTTGTAATAC
Atg2_sall_fw1	GTCGGTCCGACCAAATCCTCAGAACAACCTTACGTGTTG
Atg2_ncol_re1	GTGCCATGGCGCTCATATAAAGTGAAGTAGCCTCC
Atg2_sacI_fw3	GTCGGAGCTCAGTAAAGCGGAAGCAAGCAGTTCGAAATC
Atg2_link_xbaI_re3	GGCGTCTAGAGGACCCACCACCTCCAGAGCCACCGCCACCCG AATCAGTCCGATTGGACTTGTACTTATC
Atg2_tag_fw	AGACGCATAACGAGCAAATCAATGATAAGTACAAGTCCAATCCG ACTGATTCGTCCGGTTCTGCTGCTAG
Atg2_tag_re	TTTTAGCCGCGGTCAGTGACATTTTGGCTTTCCACCATTCCAC GTCTGAAAACCTCGAGGCCAGAAGAC
Atg9_tag_fw	GTGGTGTCTTAGGACTTGTTAAAGAGTATTACAAGAAGTCTGAC GTCGGAAGATCCGGTTCTGCTGCTAG
Atg9_tag_re	AAGGAAACAGTTATATATATAGTTATATTGGATGATGTACACGAC ACAGTCTGCCTCGAGGCCAGAAGAC
Atg18_t_fw	CGGAGAGAGGCGGCGATTGCTTAATATTGTCACAGTATTCCATC TTGATGGATTCCGGTTCTGCTGCTAG
Atg18_t_re	GTTTATATAAACTATATTGTGTATGCGTTGTGACGTACGGAAGG CAGCGCGCCTCGAGGCCAGAAGAC
Atg2_ko_fw	GATTAAAGCAAATTAAGAGGAACCCTTTTTTTTTTTGGATTCGAT ACATCCGGTTCTGCTGCTAG
Atg18_ko_fw	TTAGTAATAGTGTTCCAGTTAACTCTGTATCCTTTTCTTCTTCGG CCTGACATCCGGTTCTGCTGCTAG
Atg1_ko_fw	GCTACCCCATATTTTCAAATCTCTTTTACAACACCAGACGAGAAA TTAAGAAATCCGGTTCTGCTGCTAG

Atg1_tag_re	TTTAATGACGAACTCGTAAAGCATTTTCGAGAGTAGCATAACATA ATCATGAAGCCTCGAGGCCAGAAGAC
-------------	---

Strains

WR 619	BY Mat A his3 Δ 1 leu2 Δ 0 LYS2 met15 Δ 0 ura3 Δ 0
WR 157	BY SILAC Mat A arg4::KanMX lys1::???
yCK 481	BY Mat A atg1::HIS
WR636	BY SILAC Mat A Atg9-HTB _{eq} ::NatMX
IH 59	BY SILAC Mat A Atg9-HTB _{eq} ::NatMX atg1::HIS
IH 159	BY Mat A Atg2-HTB _{eq} ::NatMX
IH 178	BY Mat A atg1::HIS Atg2-HTB _{eq} ::NatMX
IH 185	BY Mat A atg1::HIS Atg18-HTB _{eq} ::NatMX
IH 167	BY Mat A Atg18-HTB _{eq} ::NatMX
yCK 723	Mat A atg1::KanMX atg9::KanMX
IH 227	Mat A atg1::HIS atg2::KanMX
IH 299	Mat A atg1::HIS atg18::KanMX

Plasmids

IC 18	Atg1-4xH3HA YCp33
IC 59	Atg2-linker-Suv320 YCp111
IC 35	Atg9-Suv320 YCp111
IC 2	Atg18-linker-Suv320 YCp111
pCF 7	PBS2-Suv320 YCp111
pCF 33	Sho1-4xH3HA YCp33
pAP 108	Fps1-Suv320 YCp111
pAP 149	Fps1 4xH3HA YCp33
pCK 364	Atg2-TAP pRS315
pAP 28	Suv320 YCp111
pGA 2259	NheI KanMX
pGA 2260	NheI His3MX
pCF 154	Ste20-H3HA YEp 195
pCF181	Cdc42-H3HA YEp195
pCF190	Pbs2-H3HA YEp195

Strain construction

For the construction of Atg2, Atg9 and Atg18 HTB_{eaq} tagged variants in Atg1 deficient strains and wild type strain the HTB_{eaq}::NatMX¹ cassette was amplified from a plasmid with the appropriate primers (Atg2_tag_fw, Atg2_tag_re, Atg9_tag_fw, Atg9_tag_re, Atg18_t_fw and Atg18_t_re) and subsequently transformed into the strains WR 619 and yCK 481. Except the HTB_{eaq}::NatMX for Atg9 tagging, this cassette was transformed into WR 157. Furthermore, to obtain a BY SILAC Atg9-HTB_{eaq} tagged strain with *atg1*Δ backgrounds again a His3MX6 knockout cassette was amplified with *atg1_ko_fw* and *atg1_tag_re* from the plasmid pGA 2260 and transformed into WR 636.

The double deletion strains of *atg2*Δ or *atg18*Δ with *atg1*Δ were obtained by the amplification of a KanMX deletion cassette from pGA 2259 (with *Atg2_ko_fw*, *Atg2_tag_re*, *Atg18_ko_fw* and *Atg18_t_re*) and the transformation of this cassette into yCK 481.

The deficiency for autophagy of the constructed strains was confirmed by defective Apel processing.

Plasmid construction

The plasmid Atg1-4xH3HA has been constructed as follows: The gene including 1kb of the upstream sequence was amplified from a genomic prep of BY 4741 in two fragments. By using the primers *Atg1_sphI_fw1*, *Atg1_bglII_re1*, *Atg1_bglII_fw2* *Atg1_xbaI_re2* a SphI restriction site could be added at the 5' end and the stop codon could be replaced with an XbaI restriction site. Atg1 fragment 1 was digested with SphI and BglII and Atg1 fragment 2 with BglII and XbaI. These two fragments were inserted into the vector pAP149 via the SphI and XbaI sites.

Atg9 and Atg18 were cloned into pAP108 with a similar strategy. Again the genes including 1kb of their promoter were amplified from a genomic prep of BY 4741 and inserted into pAP108 via the SphI and XbaI sites. Atg18, which is a small gene, could be amplified at once with the primers *Atg18_sphI_fw* and *Atg18_link_xbaI_re*. Because of its size Atg9 was amplified in a two step manner the primers *Atg9_sphI_fw1*, *Atg9_agel_re1*, *Atg9_agel_fw2*, *Atg9_xbaI_re2* using AgeI as restriction site for the ligation of these two fragments. In contrast to Atg1 and Atg9, the Atg18 primer was used to add a linker upstream of the XbaI site.

¹ The plasmid contains a point mutation in the TEV site therefore it cannot be used.

Atg2 is an extremely large gene so another cloning strategy had to be chosen. First Atg2 fragment 1 was amplified with Atg2_sall_fw1 and Atg2_ncol_re1, the last two cycles were done with Dream Tag to directly subclone the product into pGEMT System I (Promega). As second step Atg2 fragment 1 was cut from pGEMT with Sall and BglII and an Atg2 fragment 2 of pCK364 with BglII and BamHI to subclone them via Sall and HindIII into pBluescript (WR EC 293). Atg2 fragment 3 was amplified from genomic DNA with Atg2_sacl_fw3 and Atg2_link_xba_re3 (again adding a linker). Atg2 fragment 3 was cut with BamHI and XbaI and Atg2 fragment 1+2 with Sall and BamHI for triple ligation into pAP28.

The functionality of the constructed plasmids was checked via complementation of the appropriate deletions strains and subsequent confirmation of Apel processing.

SILAC labeling

SILAC labeling is based on a method described by Ong *et al.* [94] with the following variation: Strains carrying the protein of interest in a HTB_{eaq}-tagged version were grown in media containing either ¹³C labeled arginine and lysine or ¹²C arginine and lysine until an OD₆₀₀ of one.

Purification of HTB_{eaq} tagged proteins

The established tandem affinity purification in our laboratory is based on the method of Tagwerker *et al.* [93] with the following variations: yeast cultures were grown to OD₆₀₀ = 1 and harvested by filtration via a 0,45 µm nitrocellulose membrane. In case of autophagy induction by rapamycin cells were treated 45 minutes prior to harvesting with 0,2 ng rapamycin per ml culture. Directly after harvesting, the cells were quick frozen in liquid nitrogen. The cells were homogenized with a Freezer Mill using the following conditions: 10 minutes precooling then 7 cycles of 3 minutes breakage, with 3 minutes cooling at 15 CPS. The cells were resuspended in a denaturing Guanidium buffer (6 M Guanidine hydrochloride, 50 mM Tris (pH=8,8), 5 mM NaF, 0,1% TritonX-100, 1mM PMSF and a proteinase inhibitor cocktail (ETDA-free complete Mini)) and spun down at 14 000 rpm for 20 minutes to get rid of the cell debris. The cell extracts were incubated on Ni-Sepharose beads for five hours on a rotator. Then the beads were washed two times with urea buffer (8M urea, 50 mM Na-PO₄, 300 mM NaCl, 0,01% Tween, pH 8) and three times with the same urea buffer pH of 6,3 to get rid of any unspecific proteins. Afterwards the proteins were eluted from the beads in three washing steps with the

same urea buffer at pH 4,3 and additional 10mM EDTA. The pH of the 3 eluates was adjusted with 2 M NaCl to 8 before the eluates were incubated with streptavidin-agarose beads over night. The next day the beads were washed three times with a urea buffer containing 1% SDS (8M urea, 200mM NaCl, 100 mM Tris (pH8)) and three times with this urea buffer without SDS before the samples were delivered to mass spectrometry.

Sample preparation for the M-track

The cells were grown to the OD₆₀₀ of 0,8 to 1, then the first samples were taken and the time course was started. At every time point the OD₆₀₀ had to be measured for the latter calculation of the required amount of the 1x SDS sample buffer. The samples were spun down at 2500 rpm, 4°C for 1 minute and the cell pellets were frozen in liquid nitrogen. After the pellets were thawed on ice they were resuspended with 400µl of 1% glucose. Then 0,5 M NaOH was added in a 1:1 ratio and after 4 minutes incubation at room temperature the cells were spun down. The supernatant was removed and the pellet resuspended in 1x SDS sample buffer (amount of SDS buffer = 15xVol of samplexOD₆₀₀). As a next step the samples were boiled for 5 minutes and spun down again to collect the supernatant. The protein amount was measured with the Christian-Warburg method and 30 ng of protein were used for the SDS PAGE.

Immunoblotting for the M-track

The proteins were separated by SDS-PAGE and with wet transfer they were blotted onto a nitrocellulose membrane overnight. The blocking was done in 1% milk-PBST solution. Next, the blot was incubated 90 minutes with me3k9 antibody (1:500) and the secondary mouse antibody (1:10 000), which were dissolved in YE. For the production of YE 1g of homogenized wild type cells was resuspended in 10ml PBST and was spun down to get rid of the cell debris. Furthermore, a complete protease inhibitor cocktail was added to the supernatant before it was stored at 4°C. For use, this supernatant was diluted with the ratio of 1:5. The blot was analyzed with the ECL detection system.

Then the blot was stripped for one minute in stripping solution (32g MgCl₂·6H₂O in 80ml H₂O + 472µl acetic acid) and blocked again in 5% milk-PBST solution. The HA-antibody (1:10 000) and mouse antibody were dissolved in 1% milk-PBST solution and for 90 minutes incubated with the blot.

The mouse monoclonal me3k9 antibody as well as the HA antibody were obtained from Egon Ogris' lab.

Results

As described in the introduction of this thesis, kinase Atg1 plays a key role in the regulation of autophagy. However, its direct *in vivo* targets have not yet been clearly identified. *In vitro* studies propose Atg2, Atg9 and Atg18 as putative targets of the Atg1 kinase (Claudine Kraft, personal communications). In the work presented here, we wanted to validate these observations *in vivo*. To do so, we made use of quantitative mass spectrometry. Furthermore, we employed a protein proximity assay to detect interaction of the protein kinase with its putative targets.

Mass spectrometric analysis of Atg9 phosphorylation sites in logarithmic growing cells and autophagy inducing conditions

In vitro kinase assays suggested that Atg9 might be a target of Atg1. Also, a bioinformatic scan for Atg1 consensus motifs in Atg9 revealed S657, S831 and S948 as putative sites for Atg1 dependent phosphorylations [Claudine Kraft, personal communication]. Single point mutations as well as a combination of point mutations at all three sites lead to aberrant phenotypes in autophagic pathways.

To confirm putative Atg1 dependent phosphorylation sites of Atg9 *in vivo*, we established a phosphomap of Atg9 during logarithmic growth as well as during autophagy induced conditions. To do so, we performed a tandem affinity purification of Atg9 via a modified version of the HTB_{eq} tag (Reiter *et al.*, manuscript in preparation) from logarithmic growing yeast cultures, or alternatively from cultures that were treated with rapamycin and analyzed the modifications with mass spectrometry.

Altogether, we detected 23 phosphorylation sites on Atg9; most of them were found at serines and only four at threonines. We were able to achieve a 57,8% sequence coverage, which is high at the N- and C-terminal ends of Atg9. For the central part of the protein less coverage could be achieved probably caused by hardly accessible transmembrane domains located between the amino acids F319 and S744. Accordingly, most of the discovered phosphorylation sites were also found in the N- and C- termini of Atg9. The N-terminus of Atg9 contains S19, S26, S55, S59, S109, S122, S131, S135, S143, S144, S168, T236, S250, and the C-terminus S786, S792, T794, S802, T804, S819, S864, S899, S948, S969 (see Figure 4). The majority of the phosphorylation sites on Atg9 were detected during autophagic conditions, indicating that this factor becomes hyperphosphorylated during these conditions.

With our analysis we found phosphorylations on S831 and S948, two of the sites that have been implicated with autophagy by *in vitro* studies. Both of these phosphorylations were only found during autophagic conditions, although this result also might be explained by suboptimal sequence coverage. Unfortunately, we were not able to detect a phosphorylation at S657, the third of the *in vitro* identified phosphorylation sites (see Figure 4). This might be due to technical problems caused by the peptide sequence surrounding S657: Our standard sample preparation for mass spectrometry involves tryptic digestion of the proteins. Trypsin cleaves after arginines and lysines. Close proximity of a phosphorylation site to lysines or arginines can negatively influence the efficiency of a cleavage, leading to so called miscleaved peptides. In the case of S657, such a miscleavage would lead to a 40-residue peptide, which is a size that would be hard to detect with mass spectrometry. To find S657 we also tried to digest purified Atg9 with chymotrypsin and subtilisin, admittedly without success.

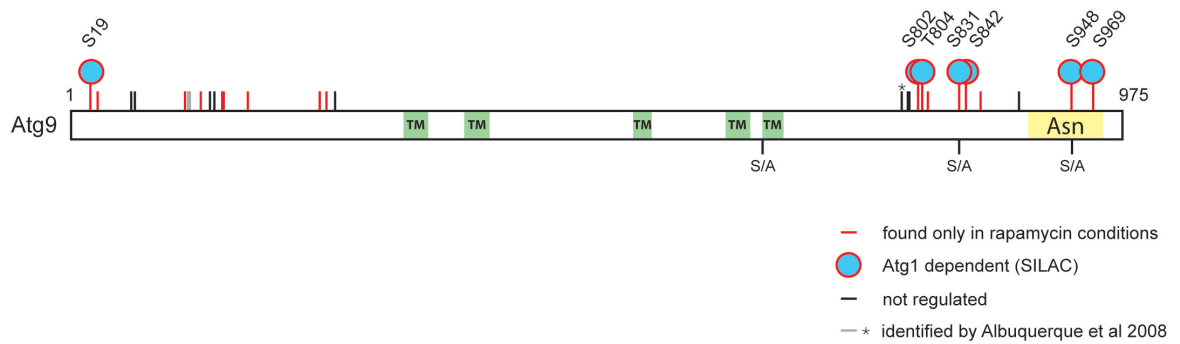
Comparison of Atg9 phosphorylation sites in Atg1 wild type and *atg1* Δ background gives first evidence for Atg1 dependent sites

To detect Atg1 regulated sites we additionally analyzed phosphorylation patterns of Atg9 purified from wild type and *atg1* Δ cells in parallel. We achieved an overlapping sequence coverage of 35% from the different strain backgrounds. These overlapping regions covered 16 of the above described phosphorylation sites of Atg9 (see Figure 4).

Four of these sites, S864, S948, S969 and T804, were only found in the Atg1 wild type background but not in the *atg1* Δ strain, indicating that the phosphorylations at these sites might be regulated by the Atg1. Phosphorylations of S864, S948 and S969 were found in the majority of the samples purified from wild type. Therefore, it is very likely that these sites are dependent on Atg1 kinase. In contrast, the phosphorylation of T804 was only found once as ambiguously allocated. Hence, this site would require more experiments to be considered as a genuine Atg1 targeted site.

Nevertheless, the possibility remains that these phosphorylation sites were just not selected for fragmentation in MS2/MS3 in the *atg1* Δ background, although they might be present in both backgrounds. To validate the observed phosphorylation sites and to determine whether the sites present in both backgrounds were regulated by Atg1 we proceeded with quantitative mass spectrometry.

A



B

```

1  MERDEYQLPN SHGKNTFLSR IFGLQSDEVN PSLNSQEMSN FPLPDIERGS
51  SLLHSTNDSR EDVDENDLRV PESDQGTSTE EEDEVDEEQV QAYAPQISDG
101 LDGDHQLNSV TSKENVLETE KSNLERLVEG STDDSVPKVG QLSSEEEEEDN
151 EFINNDGFDD DTPLFQKSKI HEFSSKKSNT IEDGKRPLFF RHILQNNRPQ
201 RDTQKLFTSS NAIHHDKDKS ANNGPRNING NQKHGTKYFG SATQPRFTGS
251 PLNNTNRFTK LFPLRKPNLL SNISVLNNTP EDRINTLSVK ERALWKWANV
301 ENLDIFLQDV YNYLGNFY CIILEKILNI CTLLFVVFVS TYMGHCVDYS
351 KLPTSHRVSD IIDKCYSNS ITGFTKFFLW MFYFFVILKI VQLYFDVQKL
401 SELQNFYKYL LNISDDELQT LPWQNVIQQL MYLKDQAMT ANVVEVKAKN
451 RIDAHDVANR IMRRENYLIA LYNSDILNLS LPIPLFRTNV LTKTLEWNIN
501 LCVMGFVFNE SGFIKQSILK PSQREFTREE LQKRFMLAGF LNIILAPFLV
551 TYFVLLLYFFR YFNEYKTPG SIGARQYTPI AEWKFREYNE LYHIFKKRIS
601 LSTTLANKYV DQFPKEKTNL FLKFVSFICG SFVAILAFLT VFDPENFLNF
651 EITSDRSVIF YITILGAIWS VSRNTITQEY HVFDPEETLK ELYEYTHYLP
701 KEWEGRYHKE EIKLEFCKLY NLRIVILLRE LTSLMITPFV LWFSLPSSAG
751 RIVDFFRENS EYVDGLGYVC KYAMFMKNI DGEDTHSMDE DSLTKKIAVN
801 GSHTLNSKRR SKFTAEDHSD KDLANNKMLQ SYVYFMDAYS NSENLTGKYQ
851 LPAKKGYPNN EGDSFLNNKY SWRKQFQPGQ KPELFRIGKH ALGPGHNISP
901 AIYSTRNPGK NWDNNNGDD IKNGTNNATA KNDDNNGNND HEYVLTESFL
951 DSGAFPNDHV IDHNKMLNSN YNGNGILNKG GVLGLVKEYY KKSVDVGR
  
```

Figure 4. **Summary of all phosphorylation sites of Atg9 found in our analysis.** The phosphomapping in (A) provides an overview of all phosphorylation sites of the Atg9 protein sequence. The exact locations are depicted in (B). All sites were mapped with a site probability score of at least 75%.

Identification of Atg1 dependent sites in Atg9 via SILAC experiments

For the quantitative phosphorylation analysis SILAC (stable isotope labeling with amino acids in cell cultures) was our method of choice. SILAC is based on supplementation of heavy and light amino acids to the media which leads to different labeling of proteins and consequently enables the simultaneous analysis of the tryptic peptide mixture. Therefore, this technology allows the quantification of the differences in the phosphorylation status of a certain protein. We simultaneously purified Atg9-HTB_{eaq} from C¹²-labeled Atg1 wild type and from C¹³-labeled *atg1*Δ cells and analyzed it by on line mass spectrometry. Except for the supply of the heavy or light labeled lysines and arginines in the media, the two strains were grown without any differences and immediately combined after harvesting. To determine the differences between the wild type background and the Atg1 deletion background during autophagic conditions, we treated both cultures with rapamycin for 45 minutes. Data of four individual experiments were combined. We were able to achieve 36% coverage of the peptide sequence of Atg9 and at first glance we observed eight sites that show differences between the wild type background and the Atg1 deletion background. Figure 5 contains a list of these peptides and also displays the extent of their phosphorylation change dependent on Atg1.

Site	Peptide	Atg1wt (¹³ C) : <i>atg1</i> Δ (¹² C)
S19	NTFLSR	no light peptide found
S802	IAVNGSHTLNSK	100*
T804	IAVNGSHTLNSK	100*
S831	MLQSYVYFMDDYSNSENLTGK	no light peptide found
S842	MLQSYVYFMDDYSNSENLTGK	25,4*
S864	GYNNEGDSFLNNK	3,5
S948	NDDNNGNNDHEYVLTEFLDSGAFPNDVIDHNK	66,2*
S969	MLNSNYNGNGILNK	no light peptide found

* peak in elution profile but no isotope pattern

Figure 5. **Atg1 dependent sites of Atg9.** The presented ratios are the results of the computational analysis. The phosphorylation sites shown in black have strong evidence to be directly regulated by Atg1.

For five peptides covering amino acids, namely S804, T804, S842, S864 and S948, relative ratios over the light (¹²C labeled) peptide were determined by quantification software (Figure 5), whereas for some phospho-peptides, namely S19, S831, and S969,

no ratios have been calculated because no light peptide was found. The absence of the light peptide can have two different reasons: first, the light peptide might not have been selected from the elution profile for subsequent fragmentation or second, no phosphorylated light form exists. The complete lack of a light peptide in the elution profile would strongly indicate that this phosphorylated site is directly and exclusively regulated by the Atg1 kinase.

To assure that the phosphorylation status at this site is indeed mediated by Atg1 and not caused by a technical artifact we reviewed the raw data (together with Verena Unterwurzacher) and checked the elution profiles of the peak of the light phosphopeptides of S19, S831 and S969. Since every peptide is eluted at a specific retention time, we compared elution profiles at the correct retention time and specific m/z values corresponding to the phospho-peptides in question. Lack of a peak for the ^{12}C labeled peptide would be a strong indication for the absence of the corresponding phosphorylated peptide in the *atg1* Δ background. As shown in Figure 6, the ^{13}C elution profiles of phospho-peptides S831 as well as of S969 show a suitable peak in the wild type sample, however the peak is absent in the *atg1* Δ sample (^{12}C), which confirms the Atg1 dependence of these sites.

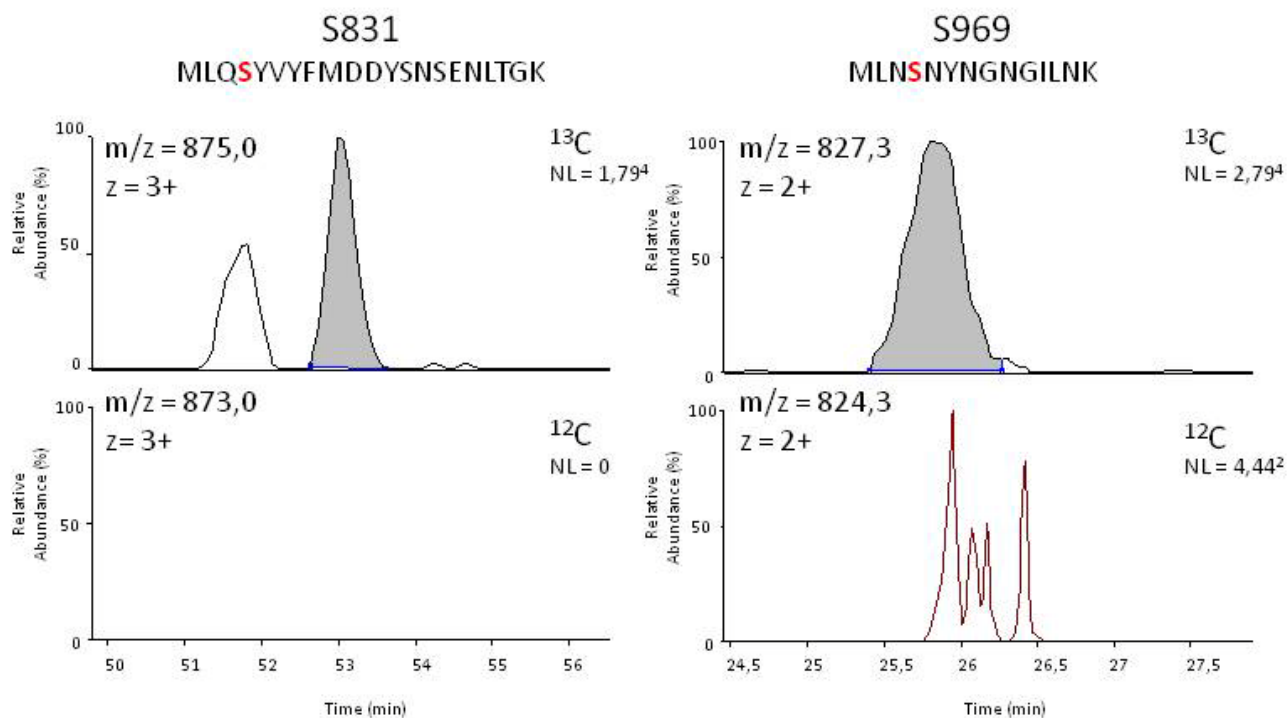
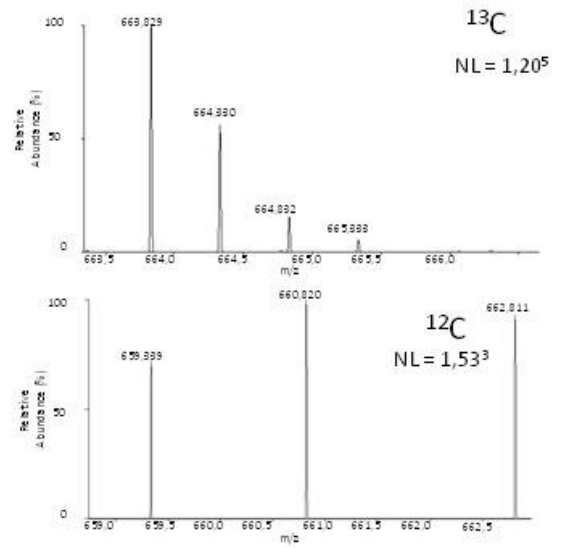
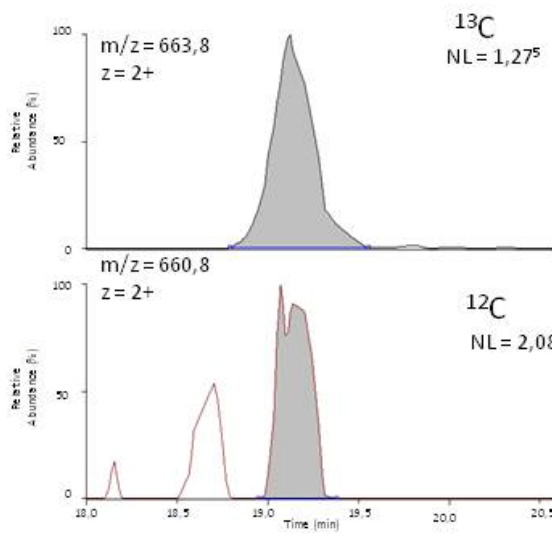


Figure 6. **Elution profile of S831 and S969.** In the elution profile only a peak for the heavy peptide but not the light is found.

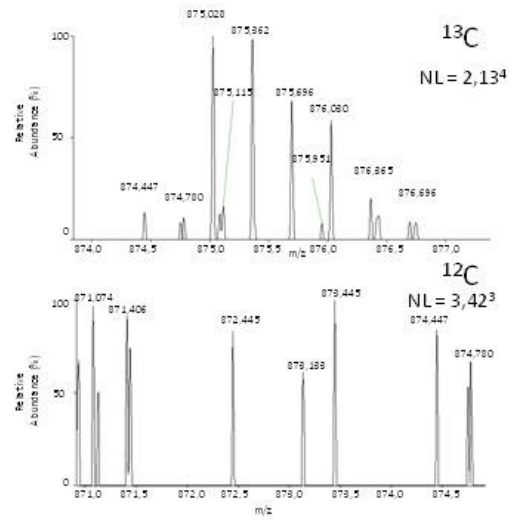
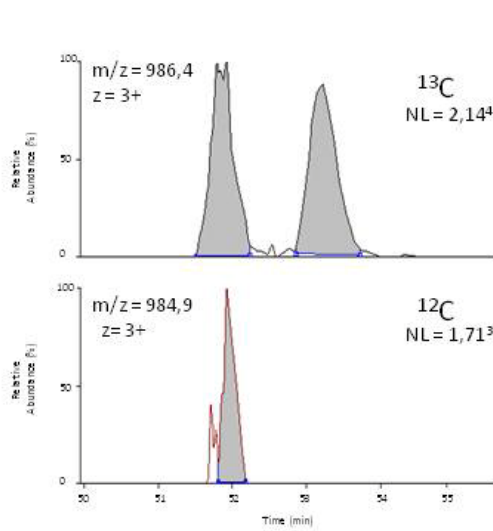
Elution profiles of the phospho-peptides covering S802, S842 and at S948 showed a possible peak for the *atg1Δ* (^{12}C) as well as for the wild type (^{13}C) labeled sample. These peaks were automatically selected and quantified by the quantification software (see Figure 7). However, manual evaluation of the isotope patterns of the light peptides showed that the automatically annotated peaks do not have the typical isotope distribution. Therefore, our manual validation of the isotope pattern of the MS2 spectra suggests that this peak originates from background noise. Therefore, no relative ratios for S802, S842 and S948 can be calculated. Thus, phosphorylation at these three sites also has to be considered as directly dependent on Atg1.

A

S802
IAVNGSHTLNSK

**B**

S842
MLQSYVYFMDDYNSENLTGK



C

S948

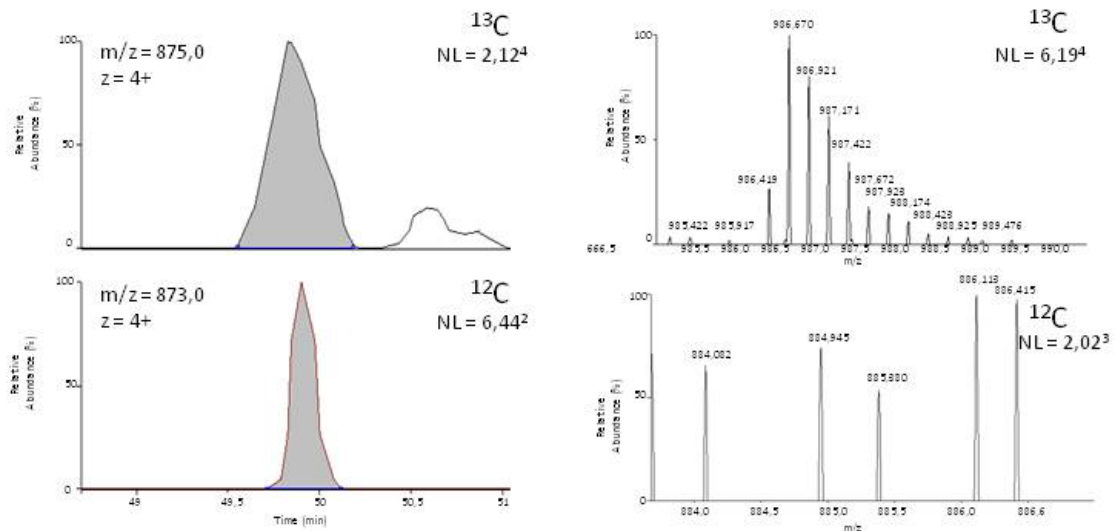
NDDNNGNNDHEYVLTE^SFLD^SSGAFP^NHDVIDH^{NK}

Figure 7. **Elution profile and isotope pattern of S802 (A), S948 (B) and S842 (C).** A typical isotope pattern (e.g. as seen in the heavy isotope pattern of S948) has the highest peak for the peptide containing only the most common ^{12}C isotope, the size of the following peak containing a mixture of ^{12}C with the heavier isotope ^{13}C decreases with increasing m/z and the peptide that contains only the ^{13}C gives the smallest peak. This figure shows that the peak in the elution profile has not the typical isotope pattern that would be seen by a corresponding peptide. This gives evidence that the peaks originate from noise.

T804 is located very close to the Atg1 dependent S802. In contrast to S802 which was found in several analyses, T804 was only identified in one of the SILAC experiments. Therefore, it remains unclear whether this site was identified due to wrong allocation of the phosphorylation site or to the variability in the selection of the targeted amino acid by the kinase. Moreover, caused by the proximity of the S802 and T804 only one heavy peak in the elution profile for both sites can be found (data not shown). Since there is no corresponding light peak for T804, this result implicates that also this phosphorylation site is absolutely dependent on Atg1.

The situation is slightly different for the phosphorylation at S19, we observed a light peak in the elution profile for phospho-peptide but no heavy to light ratio was not calculated by the automated analysis. Manual inspection of the isotope pattern did not show the appropriate distribution of the MS2 peaks; therefore the light peak most likely does not correspond to the phosphorylated peptide that was identified with the heavy peak. Therefore, we believe that the phosphorylation of S19 is also clearly dependent on Atg1 (see Figure 8).

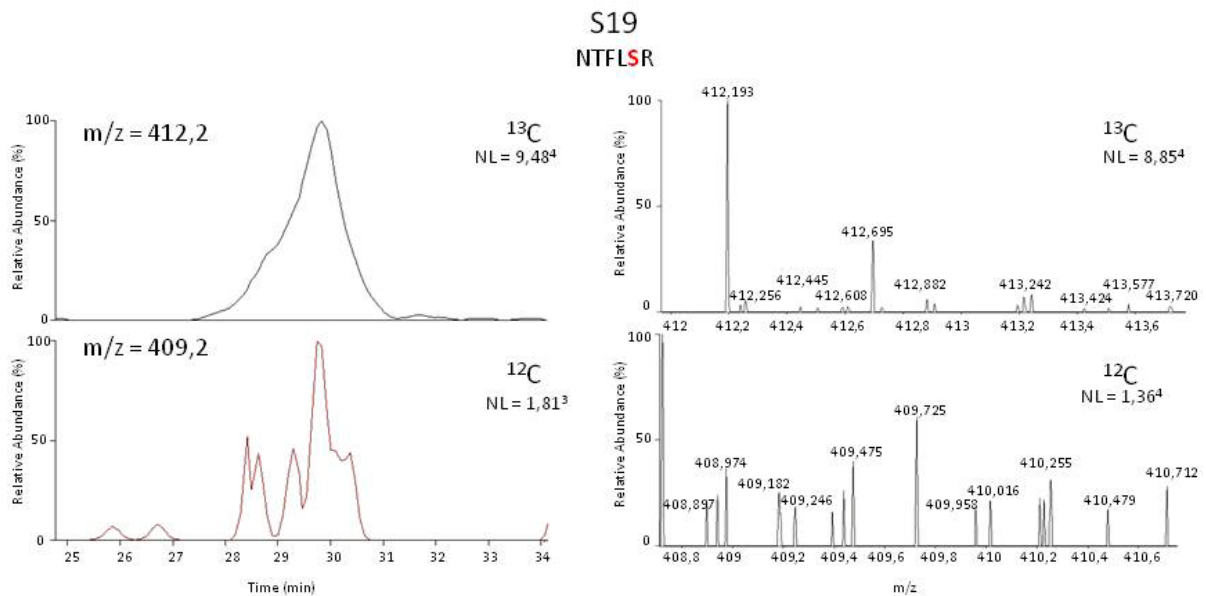


Figure 8. **Elution profile and Isotope patterns of S831.** In the elution profile (left) a light peak that is hard to quantify is seen. However, the corresponding isotope pattern does not show a natural distribution.

Taken together, we propose that our SILAC analysis identified at least six definitely Atg1 dependent phosphorylation sites on Atg9. Furthermore, we were able to corroborate Atg1 dependence of the three phosphorylation sites that have been proposed in our initial non quantitative analysis. A fourth phosphorylation site, namely S864, which according to our previous analysis was also identified as a putative Atg1 dependent site, was only found to be moderately dependent on Atg1 with a ratio of 3,5 (when wild type to an *atg1* Δ mutant was compared), even if it was strongly induced by rapamycin treatment in a wild type strain background. Therefore, we believe that this site is also phosphorylated by another kinase, because this site was found to be phosphorylated even when the kinase Atg1 is absent. We speculate that this site is either targeted by two kinases (an unknown kinase and Atg1) or phosphorylated by an unknown kinase that is hyperactivated by Atg1 during autophagic conditions. An alternative explanation would be that this phospho-site is regulated by an unknown phosphatase which becomes inactivated during autophagic conditions. Furthermore, we were able to validate two of the *in vitro* phospho-sites, namely S831 and S948.

Proposed kinase defective mutant Atg1^{K54A} still posses kinase activity

The Atg1^{K54A} mutation has been previously described as kinase defective allele of Atg1 and has already been used for experiments to gain more insight into the role and function of the Atg1 kinase. However, doubts have been raised whether this allele

expresses some residual kinase activity (Claudine Kraft, personal communication). To clarify this matter we made use of our established technologies and purified Atg9 from the generally used Atg1^{K54A} kinase defective mutant strain background and analyzed the phosphorylation pattern via non quantitative analysis. We found phosphorylations at two of the sites of Atg9 previously identified as directly dependent on Atg1, namely S802 and S969. These findings confirmed our speculation of that this kinase defective version still possesses some level of residual kinase activity.

Characterization of the Atg9-Atg1 interaction via enzymatic tagging

With our mass spectrometric approach we could show that several Atg9 phosphorylation sites are directly dependent of Atg1 kinase activity. To validate a direct interaction of these two proteins we made use of a protein-protein proximity assay based on enzymatic tagging, the so called M-track (I.Dohnal, C.Friedmann and A. Zuzuarregui). The M-tack is based on two different tags: first, the catalytic domain of the mammalian histone methyltransferase Suv39h1, which serves as donor and was fused to Atg9, and second, three repeats of a sequence of the first 21 amino acids of histone 3, which serves as an acceptor and was fused to Atg1. Interaction of donor and acceptor proteins brings the tags into close proximity allowing the transfer of the methylgroup onto the histone 3 lysine 9. This modification can be detected by western blotting using a specific antibody (see introduction).

First, we determined interaction dynamics of Atg1 and Atg9 during logarithmic growth and after autophagy induction (see Figure 9).

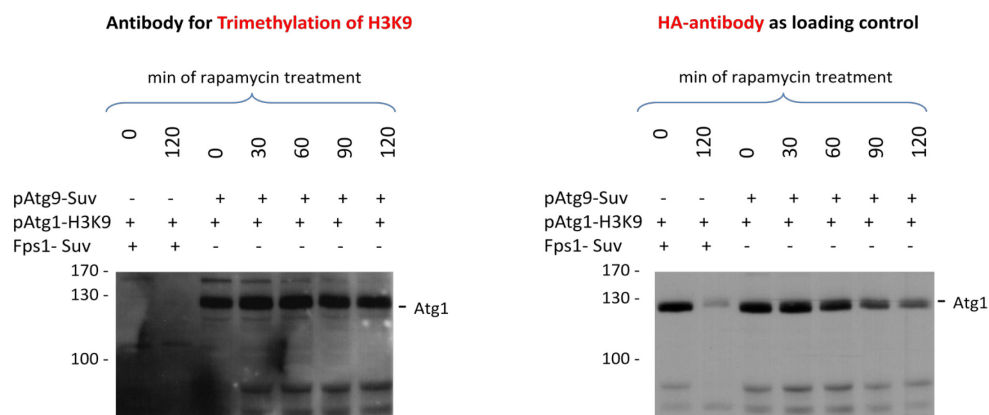


Figure 9. **M-track detecting the interaction of Atg9 with Atg1 its dynamic.** On the left side the blot for the trimethylation antibody shows a strong signal at ~130kDa. A corresponding band is also found in the HA blot, which serves as loading control.

We were able to detect a ~126kDa band with a trimethylation antibody. This band corresponds to the signal obtained with the HA antibody. Furthermore, the signal fits to the size of Atg1 including the 3xH3HA tag. Atg1 alone has a molecular weight of 101kDa. Furthermore, the trimethylation signal is absent in the Suv negative controls. Interestingly, we found that Atg1 and Atg9 strongly interact during logarithmic growth as well as at the different time points during autophagy. Since we only observed saturated signals the blot does not provide information about dynamic changes of Atg1 and Atg9 interaction.

To confirm the specificity of the Atg1-Atg9 interaction signal and to exclude the possibility that Atg9-Suv unspecifically methylates any histone 3 tagged protein, we tested whether Atg9-Suv can methylate Sho1-3xH3HA and Pbs2-Suv interacts with Atg1 (see Figure 10). Pbs2 is the MAPKK of the Hog1 MAPK pathway of *Saccharomyces cerevisiae* and Sho1 is a membrane receptor of the Hog1 pathway and both factors that are not related to autophagy. The previously established interaction of Sho1 and Pbs2 was included as a positive control.

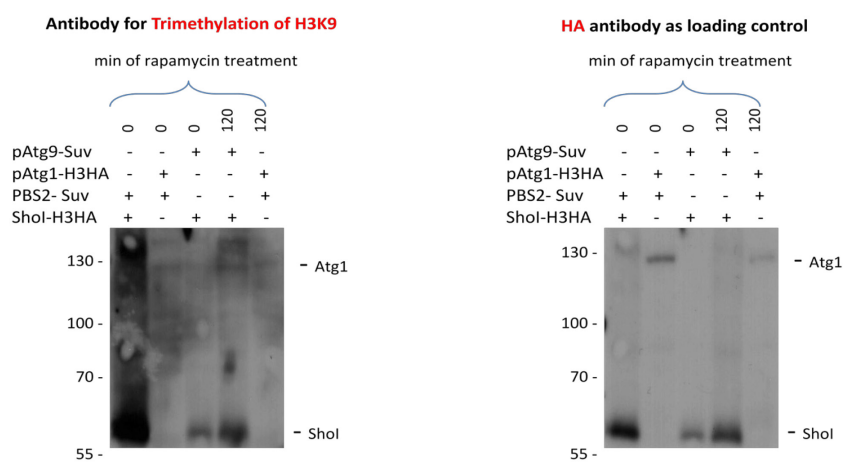


Figure 10. **M-track to determine the specificity of an interaction found by Atg9-Suv and Atg1-3xH3HA.** Atg1 is not methylated by any other Suv tagged protein while Atg9 seems to be able to interact also with other acceptors.

We observed a strong methylation signal for Sho1-3xH3HA and Pbs2-Suv, which is in line with previous studies [A. Zuzuarregui, I. Dohnal and C. Friedmann, PhD thesis]. Surprisingly, we observed an interaction signal for Atg9-Suv with Sho1-3xH3HA. There are three explanations for this observation: first, Atg9-Suv can methylate any acceptor protein in an unspecific way, or second, Atg9-Suv can easily interact with other membrane proteins or membrane associates proteins, because this sort of proteins

might share the same compartments during vesicular trafficking, or third, there is a connection between autophagy and the Hog1 pathway and Atg9 indeed interacts with Sho1 *in vivo*.

To test these hypotheses we examined whether Atg9-Suv can methylate other acceptor proteins of a pathway that is independent of autophagy (see Figure 11).

To do so, we used the membrane associated Cdc42-3xH3HA and the cytoplasmic Ste20-3xH3HA (both are factors of the Hog1 MAPK pathway). We observed no trimethylation signal for an interaction of Atg9 with Ste20 (band size including the histone tag would be around ~127kDa) but we could detect a band smear in the HA blot. However, Atg9-Suv strongly methylates the membrane associated protein Cdc42-3xH3HA (band size of 45kDa). These observations suggest that Atg9-Suv can lead to signals with membrane proteins, even if the final cellular is different, but it still specifically interacts with cytoplasmic proteins. Therefore, we believe that the methylation signal obtained with Atg1 represents a true interaction.

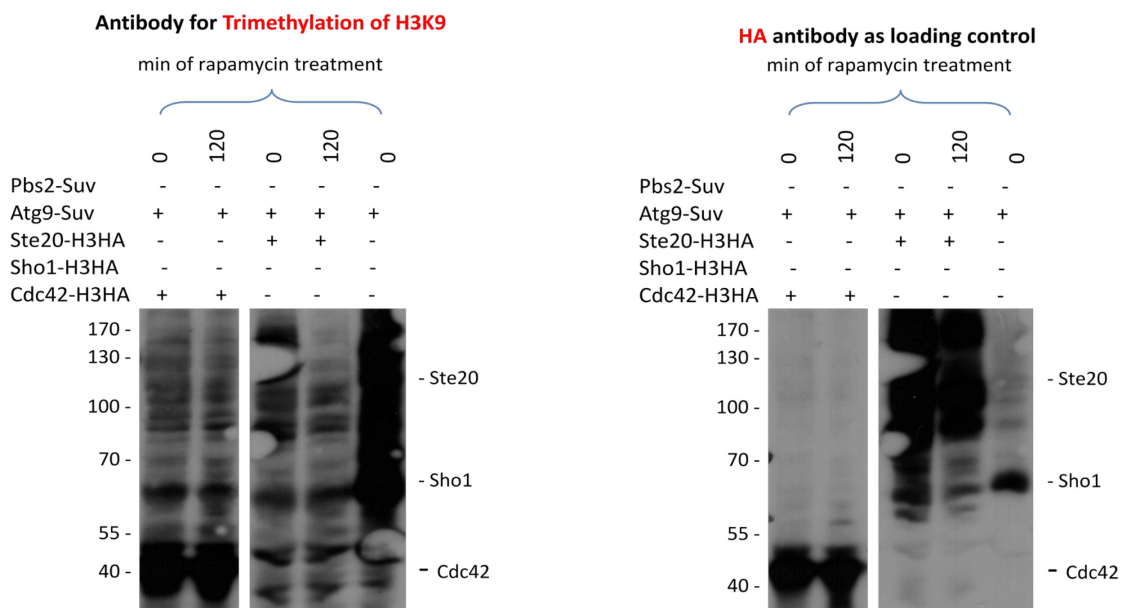


Figure 11. **M-track measuring the interaction of Atg9-Suv with different histone 3 tagged proteins.** All five lanes shown above originate from the same western blot. The blot for the trimethylation antibody shows a strong interaction for Cdc42, and less clear (considering the HA signal) no interaction for Ste20.

Currently, we set up further experiments to confirm the specificity of the Atg1 and Atg9 interaction. These experiments include the repetition of M-track with Atg1-Atg9, but this time with Atg1 containing the methylase tag and Atg9 containing the histone tag. Furthermore, we want to test whether the two proteins interact in various deletion

backgrounds, which are known to inactivate the kinase and interrupt the assembly of the Atg1 complex.

Mass spectrometric analyses of Atg2

Similar to the phosphorylation analysis of Atg9, we first used non-quantitative mass spectrometry to establish an *in vivo* phosphomap of Atg2 and to get a first insight into the changes of the Atg2 phospho-pattern during logarithmic grow as well as during autophagy. Moreover, by examining the Atg2 phospho-pattern in an *atg1* Δ strain we also obtained a first indication for which of the phospho-sites is regulated by the Atg1 kinase.

We performed four purifications of Atg2-HTB_{eq} and achieved a sequence coverage of 55,5%, which was evenly distributed throughout the whole protein. Our phosphomap of Atg2 contains 14 phosphorylation sites, except one threonine, all of them were found at serines. The majority (11 phosphorylations including the phosphopeptides of S247, S249, S940, S960, S1086, S1113, S1154, S1440, T1450, S1460, S1463) was only detected when Atg2 was purified during autophagic conditions. The remaining phospho-sites, namely S236, S624 and S954, were found in both conditions (see Figure 12).

Comparing our phosphomaps obtained from wild type background and *atg1* Δ background we achieved an overlapping sequence coverage of 40,3%. All of the 14 phosphorylations mentioned above were included in the overlapping sequence coverage, but only six of the sites, namely S246, S940, S954, S1154, T1450, S1463 were phosphorylated in the *atg1* Δ background. However, due to the limited number of purifications not all of them can be assumed to be Atg1 dependent. Furthermore, we found two additional phosphorylations at Y952 and S1443 in the *atg1* Δ background; both sites were detected during logarithmic growth and during autophagic conditions.

Because of the high sequence coverage that we obtained with each experiment we decided to proceed immediately with quantitative mass spectrometry.

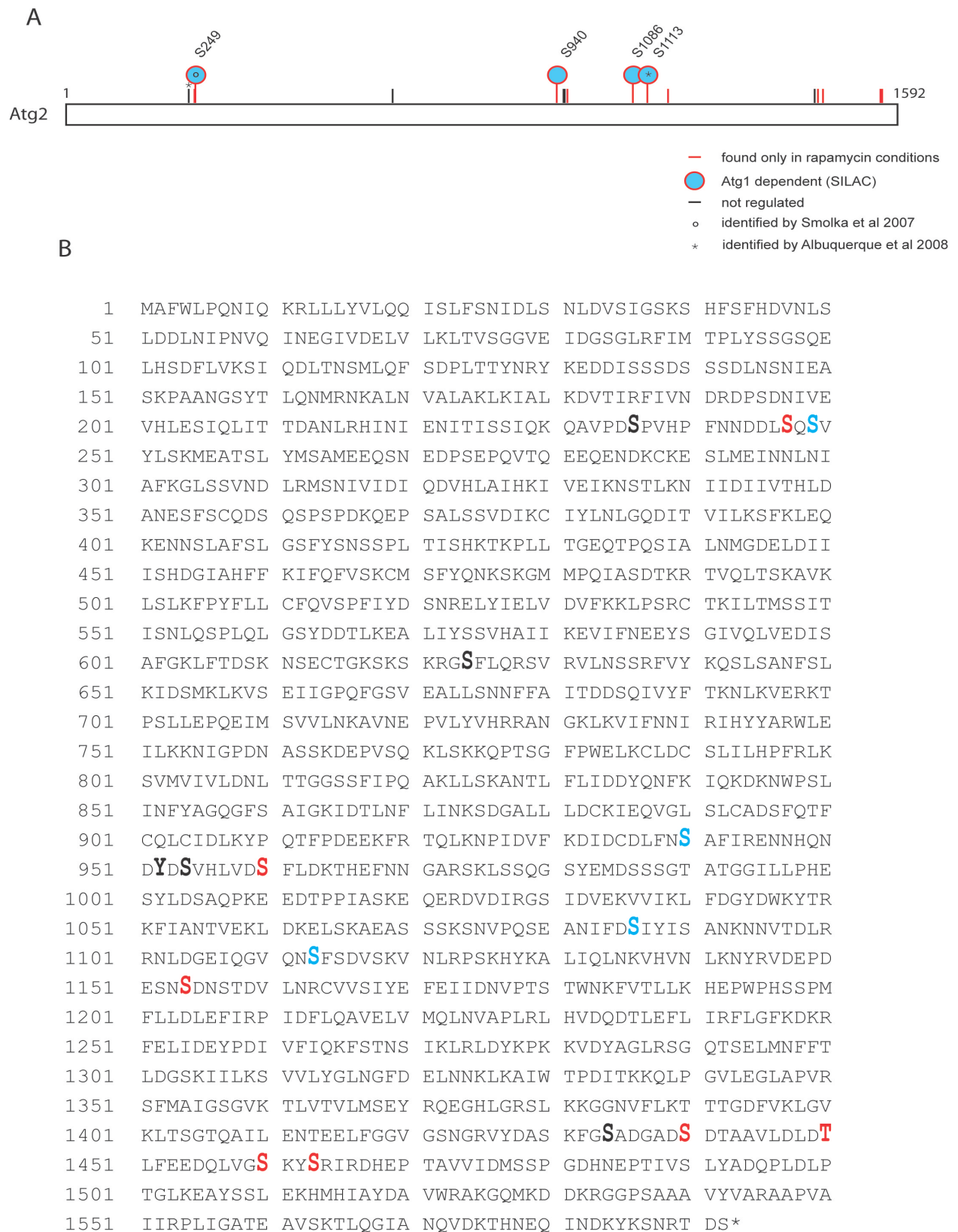


Figure 12. **Summary of all phosphorylation analyses of Atg2.** The phosphomaps in (A) provides an overview of all phosphorylation sites of the Atg2 protein sequence, including also previously identified phosphorylations. The exact locations are depicted in (B). All sites were mapped with a site probability score of at least 75%.

Identification of Atg1 targeted sites in Atg2 via quantitative mass spectrometry

Similar to Atg9, Atg2 was also identified as putative Atg1 target in vitro assays. Quantitative analysis of Atg2 phosphorylation sites *in vivo* found was performed with SILAC labeling as described above. We analyzed Atg2, which was purified simultaneously from C¹²-labeled Atg1 wild type background and from C¹³-labeled *atg1Δ* background; both strains were treated with rapamycin to induce autophagy.

Despite the fact that the data set is still preliminary (only two individual experiments have been integrated so far) the results already provide much information due to the high sequence coverage and the repeated identification of most found phosphorylation sites. We were able to cover 35,6% of the whole protein sequence of Atg2 and confirmed four Atg1 dependent phosphorylations (see Figure 13).

Site	Peptide	Atg1wt (¹³ C) : Δ <i>atg1</i> (¹² C)
S249	QAVPDSPVHPFNDDLSQ S VYLSK	22,425
S940	DIDCDLFN S AFIr	no light peptide found
S1113	NLDGEIQGVQNS S FSDVSk	35,559*
S1086	SNVPQSEANIFD S IYISANK	no light peptide found

* peak in elution profile but no isotope pattern

Figure 13. **Atg1 dependent sites of Atg2.** The presented ratios are the results of the computational analysis.

For phosphorylations on S940 as well as on S1086 no light peptide was identified by the quantification software. As described before, these results had to be manually validated (together with Verena Unterwurzacher) to assure that a phosphorylated light phospho-peptide was indeed absent and to exclude the possibility that the phospho-peptide was missed by the mass spectrometer. The elution profiles of the phospho-peptides containing S940 and S1086 (see Figure 14) show a peak for a ¹³C labeled peptide but not for a ¹²C labeled peptide. This absence of a light phosphorylated peptide in the *atg1Δ* background indicates the dependence of the phosphorylation at S940 and S1086 on the Atg1 kinase.

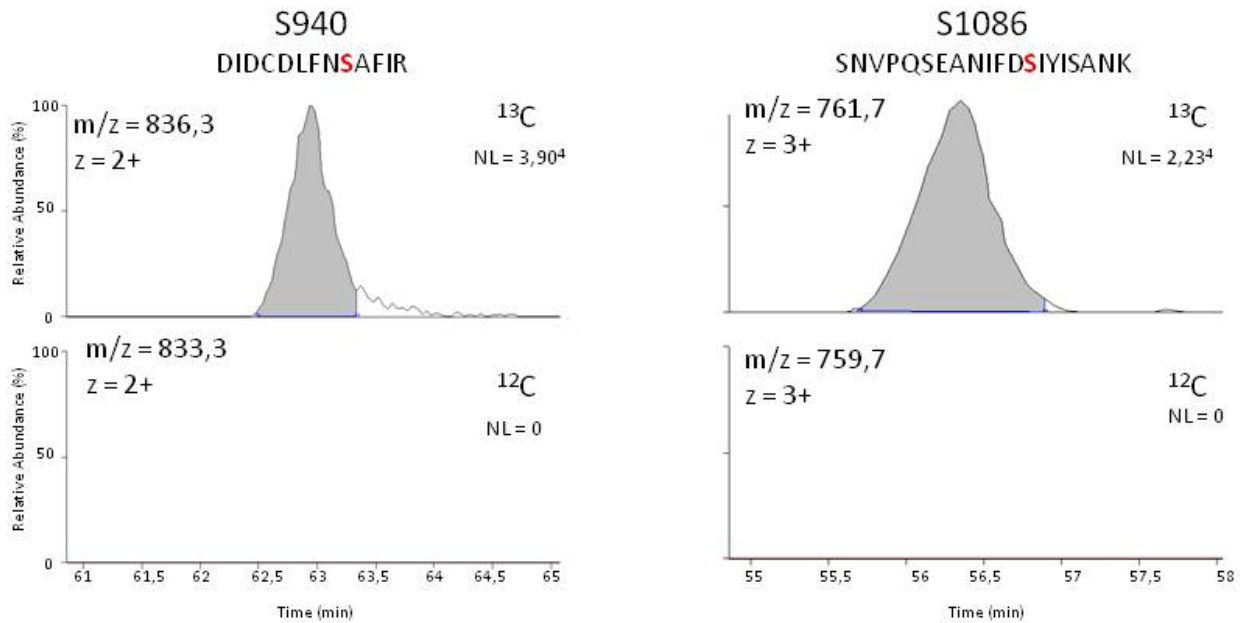


Figure 14. **Elution profiles of S940 and S1086.** A peak for the heavy phosphorylated peptides is found in both profiles whereas there is no trace of a light phosphorylated form.

For the two other putative Atg1 dependent phosphorylation sites S249 and S1113 a ratio was calculated by the quantitation software (see Figure 13). Again, we manually validated these ratios. The peak for a phosphorylation site at S1113 was also found in the elution profiles of *atg1* Δ samples in both experiments (data not shown). Similar to the phospho-serine 864 of Atg9 this site could be regulated by Atg1 and another kinase. However, as shown in Figure 15 the peak of one elution profile had no appropriate isotope pattern, whereas the other had at least one isotope pattern that possibly corresponds to a light phosphorylated peptide. Taken together, it rather seems more likely that there is no phosphorylated peptide in the *atg1* Δ background. However, for the improbable case that the one isotope pattern presents a corresponding light peptide the average ratio of the manually integrated peaks would be 66,5. Thus, the phosphorylation status of S1113 is regulated by Atg1, but the extent of this regulation remains subject of further investigations.

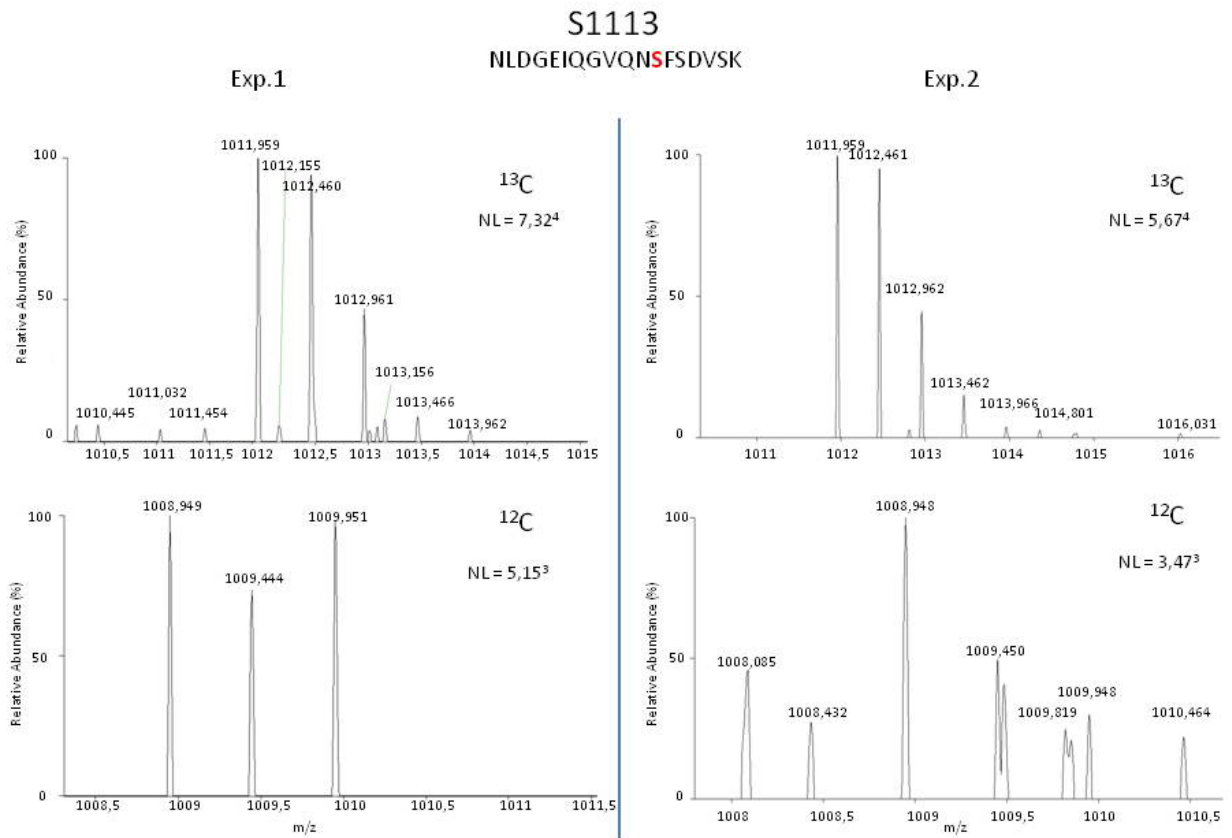


Figure 15. **Isotope patterns for S1113 from two different experiments.** On the left no typical pattern can be found whereas at least one scan of the ¹²C peptide shows typical isotope distribution (right).

The peptide containing phospho-serine 249 carries two phosphorylation sites, as shown by the two peaks in the elution profile (see Figure 16). The quantitation of the two peaks indicates that the phosphorylation status at S236 is not regulated, while the manual integration of peak A gives a ratio of 17,6 and the corresponding isotope pattern confirms the correct allocation of the phosphorylation site at S249 (see Figure 16). Admittedly, in the second experiment only the phosphorylation site at S236 could be clearly identified and for the second ambiguously allocated peptide no light peptide was found (data not shown). If this second peak belonged to the phosphorylation site on S249, this site might be regulated in an Atg1 dependent manner to a higher extent than we thought. However, the current data set indicates a role for Atg1 in the regulation of the phosphorylation site at S249.

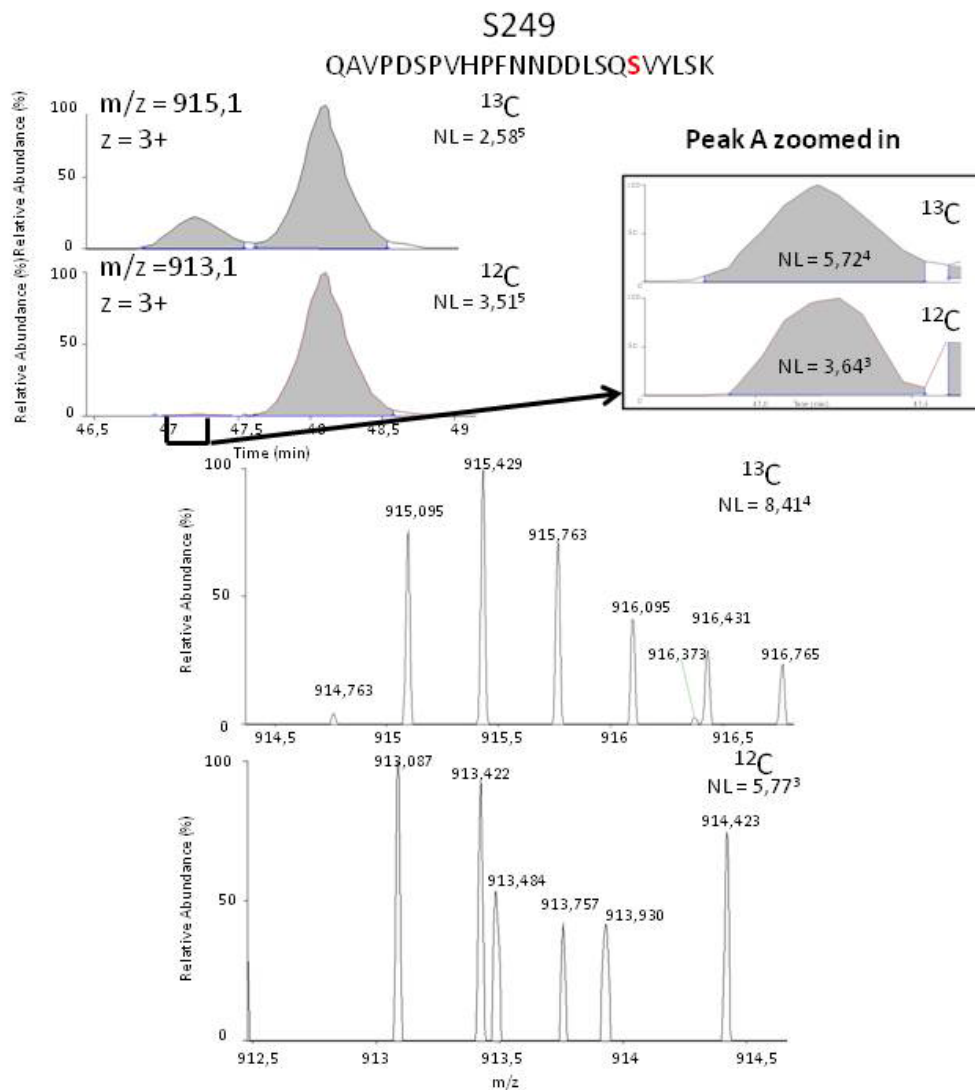


Figure 16. **Elution profile and Isotope patterns of S249.** The light corresponding peak to S249 is heightened in the box on the right. Below the both isotope patterns with an appropriate isotope distribution are shown.

Taken together, SILAC analysis enabled the discovery of possible phosphorylation sites at S249, S940, S1113, and S1086. Additionally, we could exclude 5 phospho-sites (S236, S624, S954, S1154, T1450 and S1463) to be Atg1 dependent that have previously been found in the Atg1 wild type background but not the *atg1* Δ background in our non-quantitative analysis. However, due to the size of Atg2 and the low number of experiments, more purifications are currently undertaken to obtain a more complete picture of Atg2 phosphorylation.

Determining a possible interaction between Atg1 and Atg2 - preliminary data

Based on Atg1 dependent phosphorylation sites, which were found via quantitative mass spectrometry, we assumed that Atg1 and Atg2 might interact with each other. To examine this hypothesis we again used the M-track (described above). We decided to fuse Atg2 with the donor tag und Atg1 with the acceptor tag. Producing the read out on Atg1, as in the experiments with Atg1 and Atg9, provides us the possibility to compare the intensity of the measured interactions.

To study the interaction dynamics of Atg1 and Atg2 during logarithmic growth and during autophagy, we collected samples in a time course experiments; samples were taken every 30 minutes from the time points 0 to 2h after treatment with rapamycin.

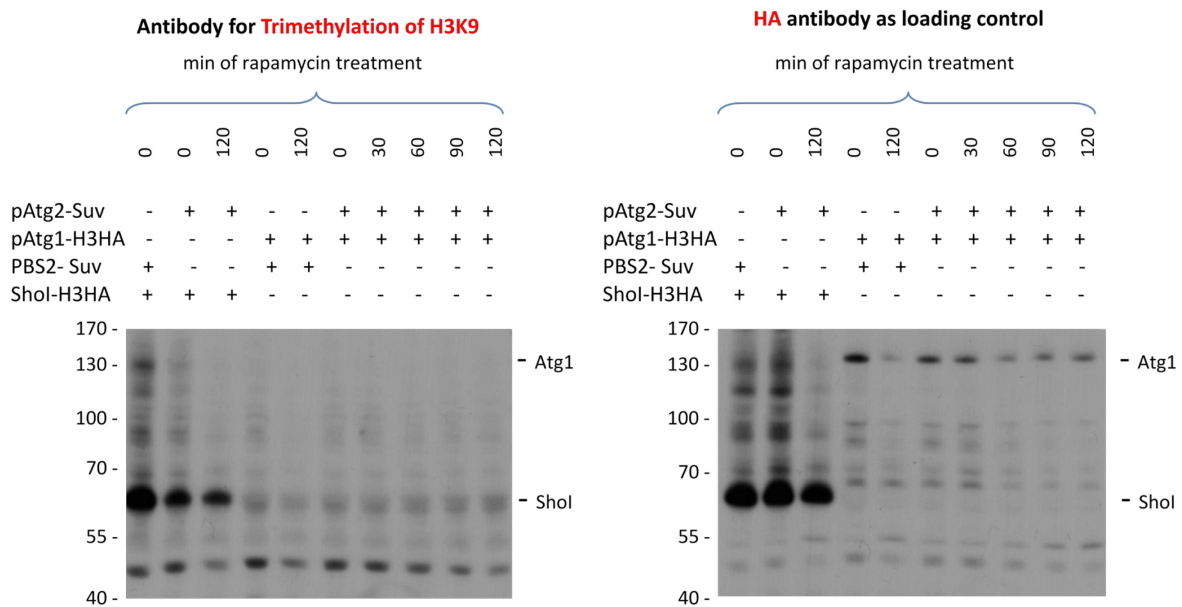


Figure 17. **M-track examining whether Atg1 interacts with Atg2.** On the trimethylation blot (left) no band at ~126 kDa is shown, whereas on the HA-blot appropriate bands are found. In contrast Sho1-3xH3HA gives a strong signal for an interaction with Atg2-Suv.

We found a HA-signal at ~126 kDa, but no corresponding trimethylation signal (see Figure 17). There are three explanation for this observation: first, there is no interaction between Atg1 and Atg2, second, the interaction between these two proteins is too transient to trimethylate a histone 3 on lysine 9, so that the trimethylation antibody fails to give a signal, or third, the tagging of both proteins on the C-terminus sterically avoids an interaction between the donor and acceptor. Interestingly, also the Atg2-Suv (similar to Atg9-Suv) gives an interaction signal with the transmembrane protein Sho1-3xH3HA. Since Atg2 associates to cellular membranes with the help of Atg18, the signal with

Sho1-3xH3HA and the lack of an interaction with the cytoplasmic Atg1 support our hypothesis that HMT tagged membrane proteins or membrane associated proteins are able to methylate other membrane proteins that are fused with the acceptor tag, but that their interaction with cytoplasmic proteins is still specific.

However, this preliminary data set has to be validated by further experiments before an Atg1 and Atg2 interaction can be excluded, especially because we got first evidences for a direct connection through the quantitative mass spectrometry.

Mass spectrometric analysis of Atg18 – preliminary data

The membrane associated protein Atg18 was the third putative Atg1 target, previously identified by *in vitro* assays. In our Atg1 consensus motif analysis of the yeast genome S219 of Atg18 gave the second best hit. However, the point mutation at this site did not result in a changed phenotype, therefore we examined whether Atg18 is targeted by Atg1 *in vivo*. Analyses of Atg18 with non-quantitative and quantitative mass spectrometry were described as already described for Atg9 and Atg2. The first couple of experiments did not provide enlightening information; therefore more intense research is required. Our non quantitative analysis revealed only three phosphorylation sites: T383 and the two unambiguously allocated S201/202 and S382/383 (see Figure 18). The phosphorylation sites on S201/202 and T393 were also found in the quantitative analysis, but their ratios of 1,3 and 0,9 indicate that these sites are not regulated by the kinase Atg1(data not shown). Furthermore, we were able to cover the peptide sequence containing S219 in our quantitative as well as in our non-quantitative analysis, but we did not detect a phosphorylation of this peptide. This data still has to be extended through the performance of further experiments.



Figure 18. **Summary of all phosphorylation analysis of Atg18.** The phosphomap in (A) shows all detected phosphorylation sites of Atg18. Their exact location is depicted in (B). The green marked regions show the total coverage of our analyses.

Examination of a possibly interaction between Atg1 and Atg18 – preliminary data

So far our mass spectrometric analysis did not show any evidence that Atg18 is targeted by Atg1. Therefore, we again decided to use the M-track (described above) to confirm Atg18 as target of the kinase Atg1.

With this assay we examined the interaction of Atg1 and Atg18 during logarithmic growth as well as during different stages of autophagy.

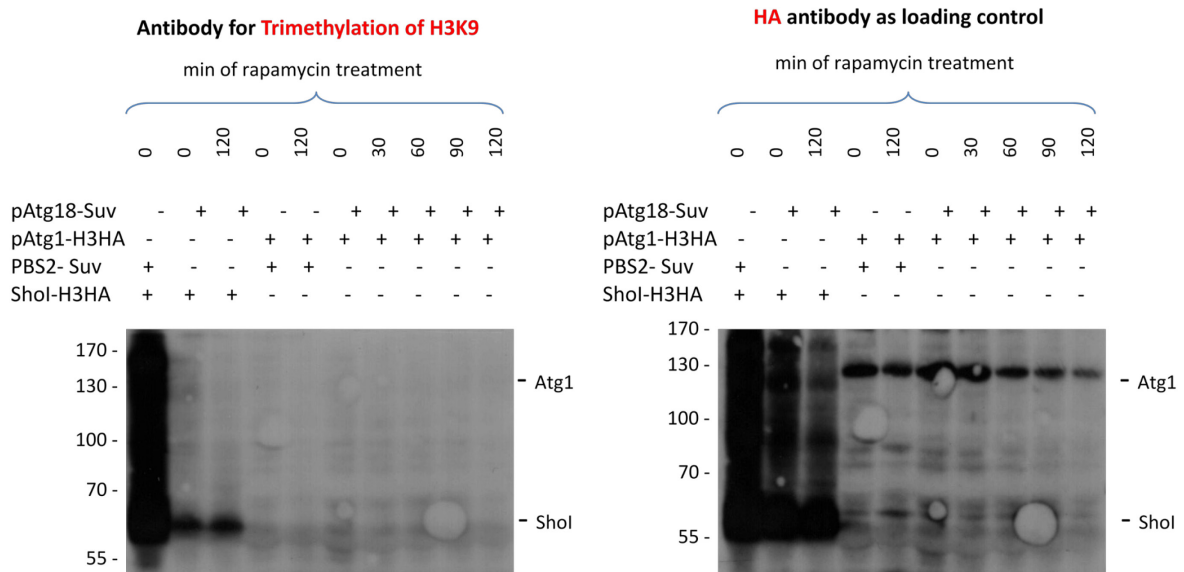


Figure 19. **M-track examining the possibility of an interaction between Atg1 and Atg18.** Comparing the absence of an Atg1 band on the trimethylation blot (left) with the strong band on the HA-blot (right) there seems to be no interaction with Atg18. However, similar to Atg9-Suv and Atg2-Suv, also Atg18-Suv also interacts with the transmembrane protein Sho1-3xH3HA.

We obtained a strong HA signal for Atg1, however a lack of a corresponding trimethylation signal indicates (similar to Atg2) a weak or no interaction between Atg1 and Atg18 or that the tags are sterically in the wrong position to interact with each other. Similar to the observations of the M-track with Atg2 and Atg9 as donor, also the membrane associating Atg18 methylates Sho1-3xH3HA, a further evidence for our hypothesis (see Figure 19). Taken together our results suggest that Atg18 is not a target of the Atg1 kinase.

Definition of an Atg1 consensus motif *in vivo*

As described above an Atg1 consensus motif has been defined based on *in vitro* assays. This motif has been used in a scan for similar sites on Atg proteins of *Saccharomyces cerevisiae*. Matches have been evaluated according to a so called similarity score (defined by scansite). S249 of Atg2 gave a similarity score of 0,3044 (a low score indicates high similarity with the motif), which was the best fit that has been detected. Moreover, preliminary data obtained by western blotting using a phospho-specific antibody raised against S249 showed a strong signal that disappeared upon phosphatase treatment (Claudine Kraft, unpublished data). These results provided further evidence that this site is indeed modified *in vivo*. Further, studies to examine the

dependence of this signal on Atg1 are currently undertaken. However, a serine to alanine substitution of this site did not lead to an autophagy relevant phenotype. We also identified S249 as Atg1 dependent in our quantitative MS analysis. However, a low induction ratio (22,4 fold induction during autophagy conditions) as well as the fact that S249 was found to be phosphorylated in an *atg1Δ* background indicates the involvement of another kinase or an indirect regulation through Atg1. Our MS analysis revealed other sites of Atg2 which better fulfilled the criteria of an Atg1 dependent site. For instance, a SILAC experiment comparing wild type to an *atg1Δ* mutant showed that serines 940 and 1086 were not phosphorylated in the Atg1 deletion strain. Compared to serine 249 these sites are clearly dependent on Atg1. Moreover, a point mutation of S1086 also did not result in an aberrant phenotype. However, we believe that such a phenotype might only be expressed when all of these sites are mutated, but combinations of point mutations have not been examined yet.

S219 of Atg18 gave the second best hit (similarity score of 0,334) in the above described scan for the Atg1 consensus motif. However, again a point mutation at this serine did not show any phenotype. Appropriately, we were not able to detect a phosphorylation at S219 in our mass spectrometric analysis, although the peptide sequence was covered in most non-quantitative and quantitative runs. Moreover, we did not find any other Atg1 dependent site on Atg18 and we were not able to detect an interaction signal between Atg1 and Atg18. All in all, the above described results raised some doubts whether the *in vitro* consensus motif is indeed recognized by Atg1 with a high affinity *in vivo*.

This doubt was further strengthened by the following observation: Serines 657, 831 and S948 of Atg9 gave higher values and therefore not ideal similarity scores (0,7252, 0,6727 and 0,7327). However, phenotypes of single point mutations and various combinations of these sites led to an autophagy aberrant phenotype. Additionally, we were able to validate S831 and S948 as direct substrates of Atg1 (unfortunately, we were not to show an Atg1 dependence of S657 due to technical difficulties). Additionally, we were able to identify four additional Atg1 regulated sites of Atg9, namely S19, S802, S842 and S969. However, similarity scores of this sites would indicate no dependence on Atg1 (0,8381, 1,2711, 1,2311 and 0,9260, respectively). Again considering the low similarity score that has been determined for some sites that have been confirmed *in vivo*, we believe that a refinement of the Atg1 consensus with using our data is necessary.

The consensus motif of Atg1 determined by *in vitro* assays can be defined as follows: The phosphorylated amino acid is a serine (hereafter defined with position 0). A hydrophobic amino acid (lysine or methionine) on the position -3, a small amino acid at position -2, a charged amino acid at position -1 and a hydrophobic amino acid (like isoleucine, valine or tyrosine) at positions +1 and/or +2 are preferred. The consensus motif obtained by our *in vivo* analysis possesses some similarity with the above described motif. For our analysis we used ten sites on Atg2 and Atg9, which were chosen, because they are definitely dependent on Atg1. Similar to the above described motif all sites were phosphorylated at a serine. Furthermore, the similarities include a preference for a hydrophobic amino acid like lysine or methionine (or valine) at position -3 and a tyrosine at position +2. Instead of a small amino acid at position -2 of the *in vivo* consensus motif contains a hydrophobic amino acid like phenylalanine or leucine at -2. There is also a lower preference for hydrophobic amino acids at positions +1,+2 and +3. Also, the tendency for a charged amino acid at position -1 is lost, except the aspartate and glutamate that are found only with a low frequency.

Atg1 regulated sites

Sites	Sequence	Score
Atg9	S19 P N S H G K N T F L S R I F G L Q S D E V	0,8381
	S802 S L T K K I A V N G S H T L N S K R R S K	1,2711
	S831 K D L A N N K M L Q S Y V Y F M D D Y S N	0,6727
	S842 Q S Y V Y F M D D Y S N S E N L T G K Y Q	1,2311
	S948 N N D H E Y V L T E S F L D S G A F P N H	0,7327
	S969 D V I D H N K M L N S N Y N G N G I L N K	0,9260
Atg2	S249 H P F N N D D L S Q S V Y L S K M E A T S	0,3044
	S940 F K D I D C D L F N S A F I R E N N H Q N	1,0123
	S1113 L D G E I Q G V Q N S F S D V S K V N L R	0,9866
	S1086 V P Q S E A N I F D S I Y I S A N K N N V	0,5754

Atg1 consensus motif

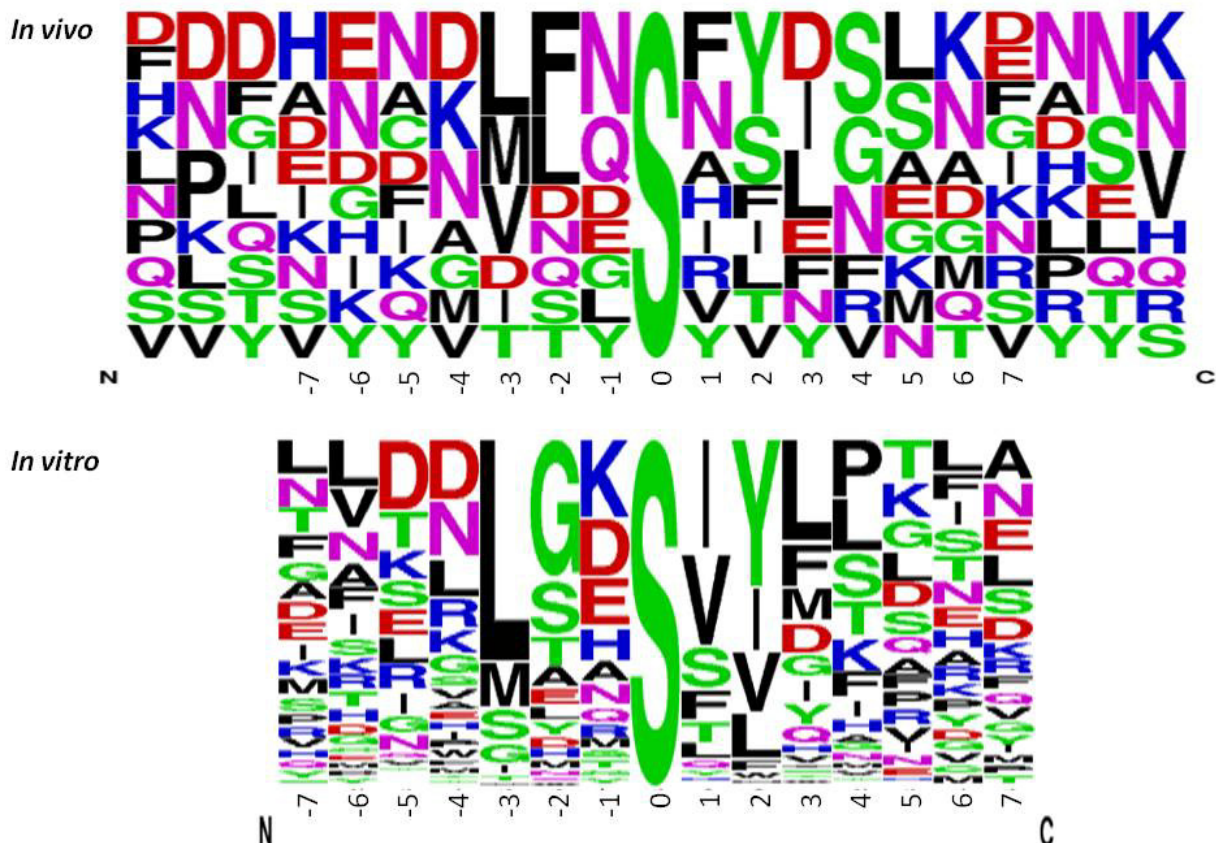


Figure 20. **Defining a new Atg1 consensus motif.** First row: all Atg1 dependent phosphorylation sites are listed with their similarity score that has been calculated by the *in vivo* consensus (score = 0 means absolute similarity). Below: the new Atg1 consensus defined by our *in vivo* methods is compared to the Atg1 consensus that has been identified by Claudine Kraft with *in vitro* methods. The negative charged amino acids D,E are shown in red, the positive charged N, K, R in blue, the polar S, T, Y, C and also G in green, N,Q in purple and the unpolar uncharged M, L, A, F, I, P, N and V in black. ClustalX and the Weblogo software of Berkeley were used to create this Figure.

When looking at the *in vivo* consensus motif of Atg1 on its own, we detected only a preference for a hydrophobic amino acid at positions -3, -2 and partly at +2. However, we neglected the possibility of folding effects. Furthermore, some of the *in vivo* Atg1 consensus motifs might bind the kinase with stronger affinity than others (therefore the consensus sequence might be “attenuated”).

To address the second problem, we sorted the sequences of our ten sites defining the *in vivo* consensus motif according to their similarity (see Figure 21). The sorting was done with the software tool “Distance Matrix” from the “Mobyly Website”. By doing so we hoped to see whether there are subsets of motifs within our group of sequences.

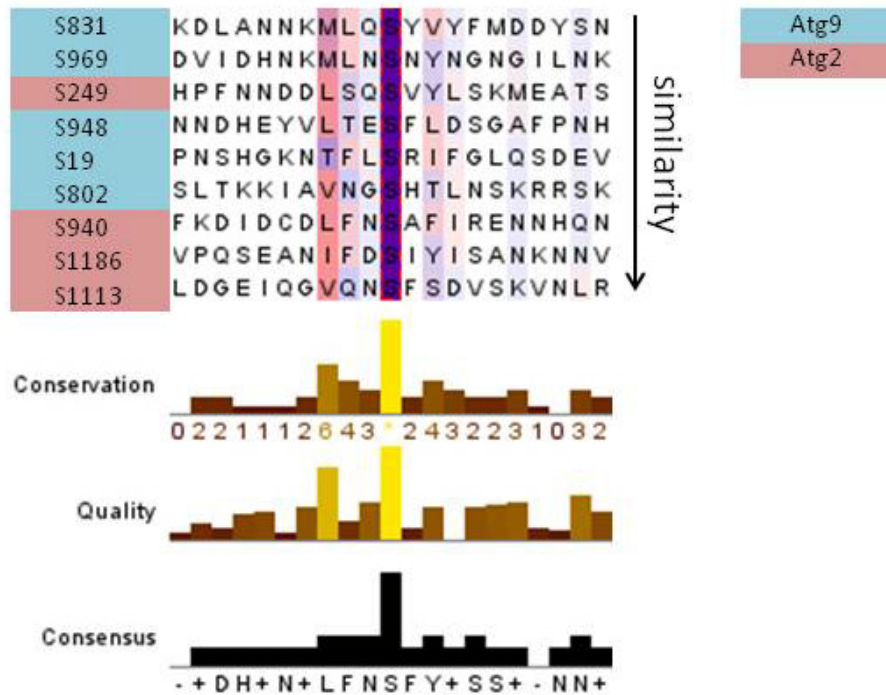


Figure 21. **Atg1 regulated sites sorted by their similarity.** Sequences at the top of this alignment have higher similarity than the ones at the bottom. The intensity of the coloured amino acids is defined by a conservation visibility score of 23. Hydrophobic amino acids are highlighted in reddish colours and hydrophilic amino acids in bluish colours.

Using Jalview we highlighted the conserved amino acids of the sorted sequences and coloured them according to their hydrophobicity. As shown in Figure 21 the Atg1 consensus has a strong tendency for hydrophobic amino acids at positions -3 and +2; the latter position seems to be less conserved (see lighter staining). Overall the sequences would have bad alignment scores (shown in the quality diagram), except for positions -3, -2, 0, and +2 (conservation scores between 4-6 and *). This is a further indication that the consensus motif which is detected by kinase Atg1 is rather weak.

Discussion

Validation of Atg1 dependent phosphorylation sites on target proteins via mass spectrometry and protein-protein interaction studies

The serine/threonine kinase Atg1 has been described to be a key regulator of autophagy. Its function and the mechanism of its activation have been thoroughly studied, but no reports on target proteins have been published until today. Recently, an *in vitro* and *in silico* analysis led to the identification of an Atg1 consensus motif. Based on sequence similarities with this consensus motif Atg2, Atg9 and Atg18 have been identified as putative Atg1 substrates. A study using *in vitro* kinase assays and point mutated variants further strengthened these observations (Claudine Kraft, unpublished data and personal communication). To answer the remaining question whether Atg1 targets these proteins also *in vivo* and whether it directly interacts with them, we used mass spectrometry and a protein proximity assay that was developed in our laboratory.

We were able to establish a detailed phosphomap of Atg9 including phosphorylations found during logarithmic growth as well as during autophagic conditions. In total we found 27 phosphorylation sites on Atg9. Furthermore, we identified six of these phosphorylation sites (S19, S802, S831, S842, S948 and S969) to be regulated by kinase Atg1. Finally, using the M-track we discovered that Atg1 and Atg9 do interact during both, rich and autophagic conditions. Therefore, we conclude that Atg9 is a direct substrate of Atg1.

The analysis of Atg2 needs further refinement, but already a number of informative results have been obtained with our mass spectrometric analysis. Altogether, we were able to map 16 phosphorylations on Atg2 and four of these phospho-sites (S249, S940, S1113, and S1086) are regulated by Atg1. Furthermore, we detected an absence of a phosphorylation signal at S940 and S1086 in the *atg1* Δ strain. This indicates a direct regulation of these serines by Atg1. Therefore, we strongly believe that Atg2 is directly targeted by the kinase. However, we could not observe a methylation signal when applying our protein-protein proximity assay. We believe that the absence of an interaction signal does not necessarily mean that Atg1 and Atg2 do not directly interact. We rather figure that the interaction might not be strong or persistent enough for a trimethylation of the acceptor tag or that steric problems such as the position of the tags interferes with the generation of the signal even when Atg1 and Atg2 interact.

Moreover, by establishing the phospho-maps for Atg2 and Atg9 we have found many phosphorylations that were only present in autophagic conditions, which indicate that additionally to Atg1 also other kinases play a role in the regulation of autophagy.

Regarding Atg18, our data still has to be considered as incomplete. Our mass spectrometric analysis of Atg18 led to the discovery of three phospho-sites, but we were not able to detect an Atg1 regulated site amongst them. Appropriately, we were not able to detect a trimethylation signal with the M-track. Although, due to the low number of purifications for our MS analysis the data of Atg18 are still preliminary, we believe that Atg18 is probably not a target of the Atg1.

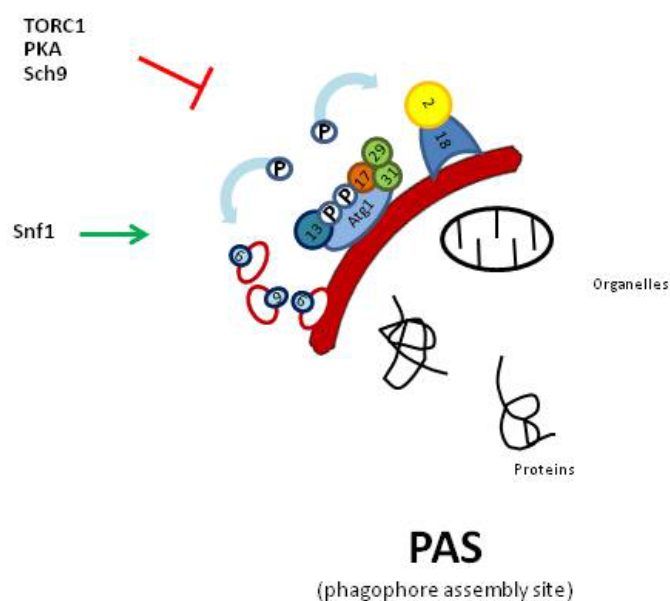


Figure 22. **The impact of our results on the actual model of autophagy.** In the initial steps of autophagy the Atg1 kinase complex, the Atg2-Atg18 complex and Atg9 localize to the PAS (Phagophore Assembly Site). Where Atg1 commits its kinase activity [11,12]. As our analyses showed the phosphorylated target proteins are Atg2 and Atg9.

The validation of Atg2 and Atg9 as substrates of Atg1 and the identification of the Atg1 dependent sites on these proteins is only the first step to deepen our understanding of the initial steps of autophagy. These results fit well into the actual model of autophagy. After receiving the nutrient signal from the TOR pathway, the Atg1 kinase complex assembles and localizes to the PAS triggering the PAS localization of other factors and complexes like the Vps34 complex, the Atg2-Atg18 complex and Atg9. As suggested by Kamada et al. and Kawamata et al. Atg1 possibly commits its kinase activity at the PAS [11,12]. Consequently, Atg2 and Atg9 would be phosphorylated after their localization to the forming autophagosome. Reggiori et al observed a block in the retrograde transport

of Atg9 in Atg1 and Atg2 deletion strains [18]. This would open the question whether the Atg1 phosphorylation of Atg2 is also required for the retrograde transport or rather for other functions of the Atg2-Atg18 complex.

Does Atg1 directly interact with its putative targets?

Additionally to the analysis of the phosphorylation patterns of Atg2, Atg9 and Atg18, this work also focused on the validation of a direct interaction of Atg1 with its putative targets.

We received a strong interaction signal for Atg1 with Atg9 during logarithmic growth as well as during autophagy. Therefore, we assume that Atg1 directly interacts or that the two factors are located in a close proximity. The strong interaction observed during logarithmic growth can be caused by basal levels of autophagy activity that can always be detected. Alternatively, the interaction could be caused by the Cvt-pathway that also requires the assembly of an Atg1 kinase complex. To our knowledge no previous studies examined the interaction between these two proteins, but interactions of Atg9 with Atg11 and Atg17 have already been described [48,95]. Both, Atg11 and Atg17, are components of the active Atg1 kinase complex; Atg11 is required for the Cvt pathway and Atg17 for autophagy. This leads to the question whether the interaction of Atg1-4xH3HA with Atg9-Suv requires Atg11 and/or Atg17.

Moreover, to assure the specificity of the interaction signal obtained with Atg9-Suv and Atg1-4xH3HA, we determined whether Atg9 also gives a trimethylation signal with other targets. Surprisingly, we found an interaction signal with Sho1-4xH3HA, a component of the (assumably unrelated) HOG MAPK pathway. We hypothesized that Sho1 and Atg9 might cause an artifact methylation signal because they come into close proximity as membrane proteins. If so, an interaction signal obtained with cytosolic proteins might still be specific. This would mean that Atg9 should not be able to methylate other cytosolic proteins; however interactions with other membrane proteins might be detectable. Indeed, we could confirm this hypothesis since with our further investigations we found an interaction signal of Atg9 with the membrane associated protein Cdc42, but no signal with the cytosolic protein Pbs2 (both proteins are also components of the HOG MAPK pathway).

We did not detect any interaction signals between Atg1 with Atg2 or Atg18, but based on our mass spectrometric results we believe that at least Atg2 is targeted by Atg1. We propose that the improper C-terminal tagging of Atg2 or the transience of the

interaction between Atg1 and Atg2 could be likely causes for the failed detection of an interaction signal. In the case of Atg18 we were not able to provide any evidence supporting its role as an Atg1 substrate, but due to the preliminary state of the data we currently cannot exclude the possibility of a connection between Atg18 and Atg1. Similar to Atg9, an interaction of Atg1 with Atg2 or Atg18 has not been described, the only identified interaction partner of the Atg2-Atg18 complex is Atg9 [18,49]. However, to confirm our hypothesis that Atg2 (but not Atg18) is a substrate of Atg1, we have to examine whether the exchange of the acceptor with the donor tag, or the tagging of the N-terminal ends, or the usage of the mono- or dimethylation antibody give rise to interaction signals.

Atg1^{K54A} defective mutant still possesses some level of activity

We examined the phosphorylation pattern of Atg9 in the Atg1^{K54A} defective mutant using mass spectrometry. The determined phosphorylation pattern included the phosphorylations at S802 and S969, which we have previously identified as direct substrates of Atg1. Therefore, we conclude that this mutant version of Atg1 still has some residual level of kinase activity. Hence, the studies of Kawamata *et al.* and Reggiori *et al.*, who used this kinase defective mutant, have to be carefully interpreted [12,18]. For example, the statement of Reggiori *et al.* which claims that Atg1 kinase activity is not required for Atg9 trafficking seems questionable. In contrast, Kawamata *et al.* also used a so called Atg1^{D211A} allele as a second control. This allele is considered to be absolutely kinase defective, but it is also uncertain whether the Atg1 kinase complex still assembles like in wild type (Claudine Kraft, personal communications). The Atg1^{D211A} mutation is located at the beginning of the activation loop [39], whereas Atg1^{K54A} is mutated at the ATP binding site (see Uniprot database). Interestingly, for both alleles the following observation has been made: Atg1 kinase activity is dispensable for the PAS localization of Atg11 and Atg29. Considering the fact that the Atg1^{D211A} gives the same results like Atg1^{K54A} also the results also obtained with Atg1^{D211A} might possibly need further validation.

Outlook

In this work we created a well defined phosphomap of Atg9 including Atg1 dependent phosphorylation and established a proximity assay for the further examination of Atg9. This makes the investigation of Atg9 or point mutated variants of this protein in different

deletion strains and with other proteins possible. Moreover, we can now determine how the deletion of components belonging to the Atg1 complex affects the interaction with Atg9. For instance, the examination of this interaction in Atg11 and Atg17 deletion strains would be interesting since these two proteins were reported to interact with Atg9. Thus, the Atg9-Atg1 interaction could be used as readout for the assembly of the Atg1 complex.

Similarly, this study provides first insights in the phosphorylation pattern of Atg2. Although this data still needs to be extended, it provides information about Atg1 regulated sites. The analysis of point mutations at these sites would be of great interest. We did not receive any signal in the M-track of Atg2 and Atg18, but further refinement of the assay can lead to more insights about the role of these two proteins. The establishment of the M-track gives us the possibility to examine further putative interaction partners and the dynamics of these interactions.

Confirming Atg2 and Atg9 as targets of Atg1 and identifying the Atg1 regulated phospho-sites provides us also the possibility to better characterize the Atg1 kinase activity and its effects on Atg2 and Atg9. This could easily be done via fluorescence microscopy. Using mutant versions of Atg2 and Atg9 carrying alanine substitutions at the Atg1 regulated phospho-sites could reveal whether Atg2 is localized to the PAS after or prior to its phosphorylation by Atg1. Moreover, examining the mutant version of Atg2 could further clarify whether the Atg1 dependent phosphorylation of Atg2 is directly connected to the retrograde transport of Atg9 or to other yet unknown functions of the Atg2-Atg18 complex.

Acknowledgements

In this section I want to thank all the people who contributed to the accomplishment of this work.

I thank Gustav Ammerer who offered me to work on this challenging project for my master theses and of course also for the support to succeed with these challenges. I want to thank Wolfgang Reiter who tried to advocate my talents and who tried to make better scientist out of me. This work would never have reached such a high quality without his help. Moreover, I am really grateful the nice working environment: Jiri Veis and Yelamanchi Syam Kumar, who had always an open ear for my problems, and Aurora Zuzuarregui, who helped me patiently to establish the M-track for the autophagic proteins. I am grateful for the enjoyable team spirit of the people from the mass spectrometric facility, especially Verena Unterwurzacher, Rainer Gith, Ilse Dohnal and Dorothea Anrather. I am thankful for my collaboration partner Claudine Kraft, whose work provided the scientific basis for this thesis and who tested my strains and plasmids for functionality. I also want to thank her for the support during the progression of my work. I want to thank Christoph Schüller, who helped me with the bioinformatic analysis. I want to thank Egon Ogris and the members of his lab of for providing the methylation antibody.

Furthermore, I thank once more Wolfgang Reiter for making this thesis comprehensible as well as to Eva Klopf and Zeljka Jandric for carefully reading the text, especially as everybody knows what a hard job this was. I also want to thank Barbara Hamilton, who recognized my passion for molecular biology and made my master's studies possible.

Finally, I want to thank my mother who always supported me in my interests and who helped financially to endure the time as student.

Literature

- [1] Melendez, A. and Neufeld, T.P. (2008) *Development* 135, 2347-60.
- [2] Li, W., Yang, Q. and Mao, Z. *Cell Mol Life Sci* 68, 749-63.
- [3] Li, W.W., Li, J. and Bao, J.K. *Cell Mol Life Sci*.
- [4] Lynch-Day, M.A. and Klionsky, D.J. *FEBS Lett* 584, 1359-66.
- [5] Xie, Z. and Klionsky, D.J. (2007) *Nat Cell Biol* 9, 1102-9.
- [6] Cebollero, E. and Reggiori, F. (2009) *Biochim Biophys Acta* 1793, 1413-21.
- [7] Yorimitsu, T., Zaman, S., Broach, J.R. and Klionsky, D.J. (2007) *Mol Biol Cell* 18, 4180-9.
- [8] Casperson, G.F., Walker, N. and Bourne, H.R. (1985) *Proc Natl Acad Sci U S A* 82, 5060-3.
- [9] Wang, Z., Wilson, W.A., Fujino, M.A. and Roach, P.J. (2001) *Mol Cell Biol* 21, 5742-52.
- [10] Mayordomo, I., Estruch, F. and Sanz, P. (2002) *J Biol Chem* 277, 35650-6.
- [11] Kamada, Y., Funakoshi, T., Shintani, T., Nagano, K., Ohsumi, M. and Ohsumi, Y. (2000) *J Cell Biol* 150, 1507-13.
- [12] Kawamata, T., Kamada, Y., Kabeya, Y., Sekito, T. and Ohsumi, Y. (2008) *Mol Biol Cell* 19, 2039-50.
- [13] Kawamata, T., Kamada, Y., Suzuki, K., Kuboshima, N., Akimatsu, H., Ota, S., Ohsumi, M. and Ohsumi, Y. (2005) *Biochem Biophys Res Commun* 338, 1884-9.
- [14] Kabeya, Y., Kamada, Y., Baba, M., Takikawa, H., Sasaki, M. and Ohsumi, Y. (2005) *Mol Biol Cell* 16, 2544-53.
- [15] Obara, K. and Ohsumi, Y. *J Lipids* 2011, 498768.
- [16] Obara, K., Sekito, T., Niimi, K. and Ohsumi, Y. (2008) *J Biol Chem* 283, 23972-80.
- [17] Webber, J.L. and Tooze, S.A. *FEBS Lett* 584, 1319-26.
- [18] Reggiori, F., Tucker, K.A., Stromhaug, P.E. and Klionsky, D.J. (2004) *Dev Cell* 6, 79-90.

- [19] Suzuki, K., Kirisako, T., Kamada, Y., Mizushima, N., Noda, T. and Ohsumi, Y. (2001) *Embo J* 20, 5971-81.
- [20] Kirisako, T. et al. (2000) *J Cell Biol* 151, 263-76.
- [21] Ichimura, Y. et al. (2000) *Nature* 408, 488-92.
- [22] Tanida, I., Mizushima, N., Kiyooka, M., Ohsumi, M., Ueno, T., Ohsumi, Y. and Kominami, E. (1999) *Mol Biol Cell* 10, 1367-79.
- [23] Shintani, T., Mizushima, N., Ogawa, Y., Matsuura, A., Noda, T. and Ohsumi, Y. (1999) *Embo J* 18, 5234-41.
- [24] Kuma, A., Mizushima, N., Ishihara, N. and Ohsumi, Y. (2002) *J Biol Chem* 277, 18619-25.
- [25] Mizushima, N., Noda, T. and Ohsumi, Y. (1999) *Embo J* 18, 3888-96.
- [26] Darsow, T., Rieder, S.E. and Emr, S.D. (1997) *J Cell Biol* 138, 517-29.
- [27] Ishihara, N. et al. (2001) *Mol Biol Cell* 12, 3690-702.
- [28] Kim, J., Dalton, V.M., Eggerton, K.P., Scott, S.V. and Klionsky, D.J. (1999) *Mol Biol Cell* 10, 1337-51.
- [29] Rieder, S.E. and Emr, S.D. (1997) *Mol Biol Cell* 8, 2307-27.
- [30] Weidberg, H., Shvets, E. and Elazar, Z. *Annu Rev Biochem* 80, 125-56.
- [31] Teter, S.A., Eggerton, K.P., Scott, S.V., Kim, J., Fischer, A.M. and Klionsky, D.J. (2001) *J Biol Chem* 276, 2083-7.
- [32] Yang, Z., Huang, J., Geng, J., Nair, U. and Klionsky, D.J. (2006) *Mol Biol Cell* 17, 5094-104.
- [33] Klionsky, D.J., Cueva, R. and Yaver, D.S. (1992) *J Cell Biol* 119, 287-99.
- [34] Yoshihisa, T. and Anraku, Y. (1990) *J Biol Chem* 265, 22418-25.
- [35] Kageyama, T., Suzuki, K. and Ohsumi, Y. (2009) *Biochem Biophys Res Commun* 378, 551-7.
- [36] Morales Quinones, M. and Stromhaug, P.E. *J Biol Chem*.
- [37] Nice, D.C., Sato, T.K., Stromhaug, P.E., Emr, S.D. and Klionsky, D.J. (2002) *J Biol Chem* 277, 30198-207.
- [38] Matsuura, A., Tsukada, M., Wada, Y. and Ohsumi, Y. (1997) *Gene* 192, 245-50.

- [39] Kijanska, M., Dohnal, I., Reiter, W., Kaspar, S., Stoffel, I., Ammerer, G., Kraft, C. and Peter, M. *Autophagy* 6, 1168-78.
- [40] Yeh, Y.Y., Wrasman, K. and Herman, P.K. *Genetics* 185, 871-82.
- [41] He, C., Baba, M., Cao, Y. and Klionsky, D.J. (2008) *Mol Biol Cell* 19, 5506-16.
- [42] Reggiori, F. and Klionsky, D.J. (2006) *J Cell Sci* 119, 2903-11.
- [43] Mari, M., Griffith, J., Rieter, E., Krishnappa, L., Klionsky, D.J. and Reggiori, F. *J Cell Biol* 190, 1005-22.
- [44] Ohashi, Y. and Munro, S. *Mol Biol Cell* 21, 3998-4008.
- [45] He, C., Song, H., Yorimitsu, T., Monastyrska, I., Yen, W.L., Legakis, J.E. and Klionsky, D.J. (2006) *J Cell Biol* 175, 925-35.
- [46] Yen, W.L., Legakis, J.E., Nair, U. and Klionsky, D.J. (2007) *Mol Biol Cell* 18, 581-93.
- [47] Tucker, K.A., Reggiori, F., Dunn, W.A., Jr. and Klionsky, D.J. (2003) *J Biol Chem* 278, 48445-52.
- [48] Sekito, T., Kawamata, T., Ichikawa, R., Suzuki, K. and Ohsumi, Y. (2009) *Genes Cells* 14, 525-38.
- [49] Wang, C.W., Kim, J., Huang, W.P., Abeliovich, H., Stromhaug, P.E., Dunn, W.A., Jr. and Klionsky, D.J. (2001) *J Biol Chem* 276, 30442-51.
- [50] Efe, J.A., Botelho, R.J. and Emr, S.D. (2007) *Mol Biol Cell* 18, 4232-44.
- [51] Nair, U., Cao, Y., Xie, Z. and Klionsky, D.J. *J Biol Chem* 285, 11476-88.
- [52] Shintani, T., Suzuki, K., Kamada, Y., Noda, T. and Ohsumi, Y. (2001) *J Biol Chem* 276, 30452-60.
- [53] Kuroyanagi, H., Yan, J., Seki, N., Yamanouchi, Y., Suzuki, Y., Takano, T., Muramatsu, M. and Shirasawa, T. (1998) *Genomics* 51, 76-85.
- [54] Yan, J. et al. (1999) *Oncogene* 18, 5850-9.
- [55] Chan, E.Y., Kir, S. and Tooze, S.A. (2007) *J Biol Chem* 282, 25464-74.
- [56] Kim, J., Kundu, M., Viollet, B. and Guan, K.L. *Nat Cell Biol* 13, 132-41.
- [57] Ganley, I.G., Lam du, H., Wang, J., Ding, X., Chen, S. and Jiang, X. (2009) *J Biol Chem* 284, 12297-305.

- [58] Mercer, C.A., Kaliappan, A. and Dennis, P.B. (2009) *Autophagy* 5, 649-62.
- [59] Itakura, E., Kishi, C., Inoue, K. and Mizushima, N. (2008) *Mol Biol Cell* 19, 5360-72.
- [60] Chen, Y. and Klionsky, D.J. *J Cell Sci* 124, 161-70.
- [61] Polson, H.E., de Lartigue, J., Rigden, D.J., Reedijk, M., Urbe, S., Clague, M.J. and Tooze, S.A. *Autophagy* 6.
- [62] Behrends, C., Sowa, M.E., Gygi, S.P. and Harper, J.W. *Nature* 466, 68-76.
- [63] Simonsen, A. et al. (2004) *J Cell Sci* 117, 4239-51.
- [64] Young, A.R. et al. (2006) *J Cell Sci* 119, 3888-900.
- [65] Mizushima, N. et al. (2003) *J Cell Sci* 116, 1679-88.
- [66] Mizushima, N. et al. (2001) *J Cell Biol* 152, 657-68.
- [67] Filimonenko, M. et al. *Mol Cell* 38, 265-79.
- [68] Tanida, I., Ueno, T. and Kominami, E. (2004) *Int J Biochem Cell Biol* 36, 2503-18.
- [69] Kimura, S., Noda, T. and Yoshimori, T. (2008) *Cell Struct Funct* 33, 109-22.
- [70] Fass, E., Shvets, E., Degani, I., Hirschberg, K. and Elazar, Z. (2006) *J Biol Chem* 281, 36303-16.
- [71] Kochl, R., Hu, X.W., Chan, E.Y. and Tooze, S.A. (2006) *Traffic* 7, 129-45.
- [72] Dunn, W.A., Jr. (1990) *J Cell Biol* 110, 1935-45.
- [73] Gordon, P.B. and Seglen, P.O. (1988) *Biochem Biophys Res Commun* 151, 40-7.
- [74] Fader, C.M., Sanchez, D.G., Mestre, M.B. and Colombo, M.I. (2009) *Biochim Biophys Acta* 1793, 1901-16.
- [75] Furuta, N., Fujita, N., Noda, T., Yoshimori, T. and Amano, A. *Mol Biol Cell* 21, 1001-10.
- [76] Jager, S., Bucci, C., Tanida, I., Ueno, T., Kominami, E., Saftig, P. and Eskelinen, E.L. (2004) *J Cell Sci* 117, 4837-48.
- [77] Tsukamoto, S., Kuma, A., Murakami, M., Kishi, C., Yamamoto, A. and Mizushima, N. (2008) *Science* 321, 117-20.

- [78] Kuma, A. et al. (2004) *Nature* 432, 1032-6.
- [79] Hara, T. et al. (2006) *Nature* 441, 885-9.
- [80] Komatsu, M. et al. (2006) *Nature* 441, 880-4.
- [81] Rabinowitz, J.D. and White, E. *Science* 330, 1344-8.
- [82] Rubinsztein, D.C., Marino, G. and Kroemer, G. *Cell* 146, 682-95.
- [83] Dengjel, J. et al. (2005) *Proc Natl Acad Sci U S A* 102, 7922-7.
- [84] Schmid, D., Pypaert, M. and Munz, C. (2007) *Immunity* 26, 79-92.
- [85] Xu, Y., Jagannath, C., Liu, X.D., Sharafkhaneh, A., Kolodziejaska, K.E. and Eissa, N.T. (2007) *Immunity* 27, 135-44.
- [86] Delgado, M.A., Elmaoued, R.A., Davis, A.S., Kyei, G. and Deretic, V. (2008) *Embo J* 27, 1110-21.
- [87] Nakagawa, I. et al. (2004) *Science* 306, 1037-40.
- [88] Birmingham, C.L., Smith, A.C., Bakowski, M.A., Yoshimori, T. and Brumell, J.H. (2006) *J Biol Chem* 281, 11374-83.
- [89] Mathew, R. et al. (2007) *Genes Dev* 21, 1367-81.
- [90] Liang, X.H., Jackson, S., Seaman, M., Brown, K., Kempkes, B., Hibshoosh, H. and Levine, B. (1999) *Nature* 402, 672-6.
- [91] Carew, J.S. et al. (2007) *Blood* 110, 313-22.
- [92] Degenhardt, K. et al. (2006) *Cancer Cell* 10, 51-64.
- [93] Tagwerker, C. et al. (2006) *Mol Cell Proteomics* 5, 737-48.
- [94] Ong, S.E., Blagoev, B., Kratchmarova, I., Kristensen, D.B., Steen, H., Pandey, A. and Mann, M. (2002) *Mol Cell Proteomics* 1, 376-86.
- [95] Chang, C.Y. and Huang, W.P. (2007) *Mol Biol Cell* 18, 919-29.

Curriculum vitae

Isabella Hansmann Bakk.
Engerthstraße 99/10/9
A-1200 Vienna
Tel. +43 (0) 699 / 17275828

Personal Data

Date of Birth: 04.09.1987

Place of Birth: Vienna, Austria;

Father: Bernhard Hansmann, Dentist;

Mother: Ursula Hansmann, Sales Representative of a financial company;

Education

1993-1994 Preschool in Baden;
1994-1998 Elementary school in Baden;
1998-2002 Secondary school in Berndorf;
2002-2006 Upper school in Vienna;
2006-2009 Bachelor study of Nutrition Sciences at the University of Vienna
2009-2012 Master study of Molecular Biology at the University of Vienna

Internships

- September 2009 internship in the quality control laboratory of the meat product industry Berger GmbH (microbiology and chemical rapid analysis of food) (Sieghartskirchen, Austria)

- February 2010 internship in the group of Prof. Ammerer at the Department of Biochemistry and Cell biology (MFPL) (Vienna, Austria)

- Juni/Juli 2010 internship in the group of Prof. Penninger at the IMBA (Vienna, Austria)

- October/November 2010 internship in the group of Dr. Alison Butt at the Garvan institute (Sydney, Australia)